รายงานวิจัยฉบับสมบูรณ์

โครงการ ผลจากการเปลี่ยนชนิดกรดอะมิโนต่อประสิทธิภาพการยึดจับระหว่างฮีมแมกกลูตินิน H1N1 สายพันธุ์ต่าง ๆกับตัวรับในมนุษย์: การศึกษาทางทฤษฎี

(Effects of Amino Acid Changes on Human Receptor Binding Efficiency of Different H1N1 Hemagglutinins: Theoretical Study)

โดย นางสาวณัฏฐาเนตร นันทบุตร และคณะ

1 กันยายน 2553

สัญญาเลขที่ MRG5180298

รายงานวิจัยฉบับสมบูรณ์

โครงการ ผลจากการเปลี่ยนชนิดกรดอะมิโนต่อประสิทธิภาพการยึดจับระหว่างฮีมแมกกลูตินิน H1N1 สายพันธุ์ต่าง ๆกับตัวรับในมนุษย์: การศึกษาทางทฤษฎี

(Effects of Amino Acid Changes on Human Receptor Binding Efficiency of Different H1N1 Hemagglutinins: Theoretical Study)

นางสาวณัฏฐาเนตร นันทบุตร
ภาควิชาเคมี คณะวิทยาศาสตร์
มหาวิทยาลัยมหาสารคาม

สนับสนุนโดยสำนักงานคณะกรรมการการอุดมศึกษา และสำนักงานกองทุนสนับสนุนการวิจัย

(ความเห็นในรายงานนี้เป็นของผู้วิจัย สกอ. และ สกว. ไม่จำเป็นต้องเห็นด้วยเสมอไป)

CONTENTS

Project: MRG5180298

Project Title: ผลจากการเปลี่ยนชนิดกรดอะมิโนต่อประสิทธิภาพการยึดจับระหว่างฮีมแมกกลูตินิน H1N1 สายพันธุ์ต่างๆกับตัวรับในมนุษย์: การศึกษาทางทฤษฎี

Effects of Amino Acid Changes on Human Receptor Binding Efficiency of Different H1N1 Hemagglutinins: Theoretical Study

Investigator: Dr. Nadtanet Nunthaboot, Chemistry Department, Faculty of Science, Mahasarakham University

E-mail Address: nadtanet@gmail.com

Project Period: 2 years

บทคัดย่อ

การแพร่ระบาดของเชื้อไวรัสไข้หวัดใหญ่สายพันธุ์ใหม่ 2009 H1N1 ได้ก่อให้เกิดความหวาดกลัวและกลายเป็นปัญหาสำคัญระดับโลก เนื่องจากอาจก่อให้เกิดการระบาดใหญ่อย่างรุนแรง และอาจทำให้มีผู้เสียชีวิตจำนวนมาก กระบวนการแพร่พันธุ์ของเชื้อไวรัสไข้หวัดใหญ่ในมนุษย์เริ่มต้นจากการยึดจับระหว่างไกลโคโปรตีนฮีมแมกกลูตินินและตัวรับที่มีอนุพันธ์ของน้ำตาลกาแลกโทสแบบแอลฟา 2,6 (SIA-α2,6Gal) งานวิจัยนี้ได้สร้างแบบจำลองโครงสร้างสามมิติของสารประกอบเชิงซ้อนระหว่างฮีมแมกกลูตินินของเชื้อไวรัสไข้หวัดใหญ่สายพันธุ์ใหม่ 2009 H1N1 และตัวรับ SIA-α2,6Gal โดยใช้เทคนิคโฮโมโลยีโมเดลลิงและโมเลคิวลาร์ไดนามิกส์ซิมุลชัน พบว่าลักษณะทางโครงสร้างรวมทั้งอันตรกิริยาที่สำคัญมีลักษณะคล้ายกับที่พบในฮีมแมกกลูตินิน H1N1 ของสายพันธุ์อื่นๆที่มีการรายงานแล้ว อย่างไรก็ตามเพื่อให้เข้าใจมากยิ่งขึ้นถึงอิทธิพลของกรดอะมิโนในบริเวณก่อกัมมันต์ที่มีผลต่อการยึดจับระหว่างฮีมแมกกลูตินินและตัวรับ จึงได้ทำการจำลองพลวัติของสารประกอบเชิงซ้อนระหว่าง SIA-α2,6Gal กับฮีมแมกกลูตินินสายพันธุ์ใหม่ 2009 เปรียบเทียบกับสายพันธุ์ที่มีการระบาดอย่างรุนแรง (สายพันธุ์ 1918) สายพันธุ์ที่ไม่มีการระบาด (สายพันธุ์ 1930) และสายพันธุ์ที่เป็นไข้หวัดใหญ่ตามฤดูกาล (สายพันธุ์ 2005) พบว่ากรดอะมิโนที่มีประจุ ได้แก่ K145 และ E227 ที่พบในฮีมแมกกลูตินินสายพันธุ์ใหม่ 2009 มีส่วนช่วยเพิ่มประสิทธิภาพในการยึดจับกับตัวรับ โดย K145 สร้างไลซีนเฟนส์กับกรดอะมิโนไลซีน K133 K156 และ K222 ส่วน E227 ทำหน้าที่สเตบิไลซ์โครงสร้างของ K222 ให้สามารถยึดจับกับ SIA-α2,6Gal ได้ ในขณะที่ไม่พบอันตรากิริยาเหล่านี้ในฮีมแมกกลูตินินสายพันธุ์อื่นๆ นอกจากนี้การกลายพันธุ์ของกรดอะมิโน G225 เป็น D225 ที่พบในฮีมแมกกลูตินินสายพันธุ์ 1918 และ 2009 ยังช่วยเพิ่มประสิทธิภาพในการยึดจับกับตัวรับให้ดียิ่งขึ้น เนื่องจากสามารถสร้างพันธะไฮโดรเจนกับตัวรับได้ดีกว่าในกรณีของ G225 ซึ่งพบในสายพันธุ์ 1930 และ 2005 ผลการวิเคราะห์นี้สอดคล้องกับข้อมูลการทดลองที่มีการรายงานมาแล้ว ลักษณะเด่นของฮีมแมกกลูตินินสายพันธุ์ 2009 คือกรดอะมิโนในบริเวณที่มีการยึดจับกับตัวรับมีความเป็นขั้วสูงขึ้น ซึ่งน่าจะเป็นวิวัฒนาการที่แตกต่างจากไวรัสสายพันธุ์

1918 1930 และ 2005 คณะผู้วิจัยหวังเป็นอย่างยิ่งว่าข้อมูลที่ได้จากงานวิจัยนี้จะเพิ่มความรู้ความเข้าใจมากยิ่งขึ้นเกี่ยวกับกระบวนการหรือกลไกการแพร่พันธุ์ของเชื้อไวรัสไข้หวัดใหญ่สายพันธุ์ใหม่ 2009 ตลอดจนใช้เป็นข้อมูลในการติดตามการกลายพันธ์หรือการอุบัติขึ้นของไข้หวัดสายพันธุ์หม่ ในปีต่อๆ ไปอีกด้วย

คำหลัก เชื้อไวรัสไข้หวัดใหญ่ H1N1 ฮีมแมกกลูตินิน ตัวรับในมนุษย์ โมเลคิวลาร์ไดนามิกส์ซิมุเลชัน

Abstract:

The recent outbreak of the novel 2009 H1N1 influenza in humans has focused global attention on this virus which could potentially have introduced a more dangerous pandemic of influenza flu. In the initial step of the viral attachment, hemagglutinin (HA), a viral glycoprotein surface, is responsible for the binding to the human SIA α2,6 linked sialopentasaccharide host cell receptor (hHAR). In this work, the complex structure of the 2009 H1N1 HA bound to the hHAR was constructed using homology modeling and molecular dynamic simulations. The receptor was found to fit very well within the HA binding pocket. Key interactions between HA and hHAR are well conserved. The results are similar to the hHAR binding to H1 HA subtype, but are slightly different from those of H3, H5 and H9 HAs. To further understand the effects of amino acid changes in the receptor binding pocket of different strains of HA, molecular dynamics simulations of the four different HAs of Spanish 1918 (H1-1918), swine 1930 (H1-1930), seasonal 2005 (H1-2005) and a novel 2009 (H1-2009) H1N1 bound to the hHAR, were conducted and compared. The simulated results indicated that introduction of the charged HA residues K145 and E227 in the 2009 HA binding pocket was found to increase the HA-hHAR binding efficiency in comparison to the three previously recognized H1N1 strains. A positively charged K145 in the HA of a novel H1-2009 can potentially make a lysine fence with residues K133, K156 and K222 and thus provides an optimal contact to hydrogen bond with the SIA1 of the hHAR. Residue E227 stabilizes the orientation of K222 to form hydrogen bond with hHAR. Moreover, changing of the non-charged HA G225 residue (1930 and 2005) to a negatively charged D225 (1918 and 2009) provides a larger number of hydrogen bonding interactions. This finding agrees well with the experimental data. The increase in hydrophilicity of the receptor binding region is apparently an evolution of the current pandemic flu from the 1918 Spanish,

1930 swine and 2005 seasonal flues. Detailed analysis could help the understanding of how different HAs effectively attach and bind with the hHAR and could be useful for future study of the new emerging of influenza viruses.

Keywords: Influenza virus, H1N1, Hemagglutinin, Human receptor, Molecular dynamics simulations

1. **Executive summary**

A global outbreak caused by a swine origin 2009 A (H1N1) influenza virus has rapidly spread and encircled over hundred countries worldwide, causing more than 18,000 human deaths.[1] The World Health Organization (WHO) has declared as a new strain of influenza virus pandemic.[1, 2] Fear is arisen because the mutation of this strain of influenza virus could lead to a potentially more pathogenic in the near future. The pandemic H1N1 2009 is not the first human pandemic caused by H1N1 influenza virus. The most devastating influenza pandemic, 1918 H1N1 Spanish Flu, killed more than 40 million people worldwide.[3-5]

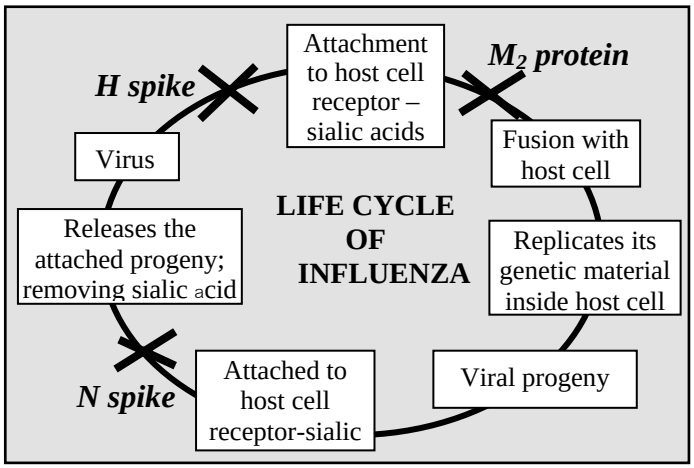

Figure 1. Influenza viral replication life cycle

Among the known targets determining the virus life's cycle, the initial step of viral attachment is mediated by the viral surface homotrimeric glycoprotein hemagglutinin (HA) binding the virion to the host cell receptor (Figure 1). Therefore, HA is an important target for the development of both vaccines and antiviral drugs against influenza viruses. Each monomer of the homotrimer is composed of two subunits, HA1 and HA2. While HA1 is known to be responsible for the viral attachment to host cell, HA2 is associated with the release of the viral RNA complexed with the RNA polymerase, through membrane fusion, [6-9] and thus HA is

essential to both host cell targeting and cell entry (infection). HA1 binds to host cell membrane receptors, glycans containing the terminal sialic acid which are attached to surface membrane proteins or lipids.[8,10,11] The specific topology, determined principally but not exclusively by the specific linkage of the terminal sialic acid to the galactose subunit and the glycan chain length, identifies the species and tissue specificity and avidity of binding, and thus its infectability and transmission rates.[12] The avian influenza virus preferentially recognizes the sialic acid α2,3 galactose (SIA-α2,3-GAL) linkage with a short glycan chain and cone like topology, while the adopted sialic acid α-2,6,galactose linkage is more favorable in both human and swine influenza viruses with longer glycan chains and an umbrella like topology.[12-16] It is supposed that the alternation in host specificity of sialic acid linked to galactose from α2,3 to α2,6,- linkage is a major barrier for influenza viruses to cross species barriers and adapt to new hosts. [9, 12, 17-20]

From the available information, it is clear that the binding domain of HA with the glycan receptors is comprised of several key structural components including the 190 helix, 130- and 220-loop domains and several other conserved residues (Figure 2) that give species and tissue specificity[11]. However, how this is derived is not clear and to date, the H1N1-2009 HA structures, either as free form or receptor bound conformation, have not yet been experimentally solved. Recently, the theoretically modeled structure of HA-receptor complex has been published[21]. However, it represents a static view of protein-receptor interactions without dynamics capture of time-dependent properties. **Therefore, in the first part of this work, structure of a novel H1N1 HA complexed with the human cell receptor, α2,6 linked sialopentasaccharide (SIA-α2,6-GAL;hHAR) was constructed. Molecular dynamics (MD) simulation was consequently performed on the homology**

modeled structure to investigate the fundamental structural characteristics, the role of conserved binding residues and receptor binding specificity.

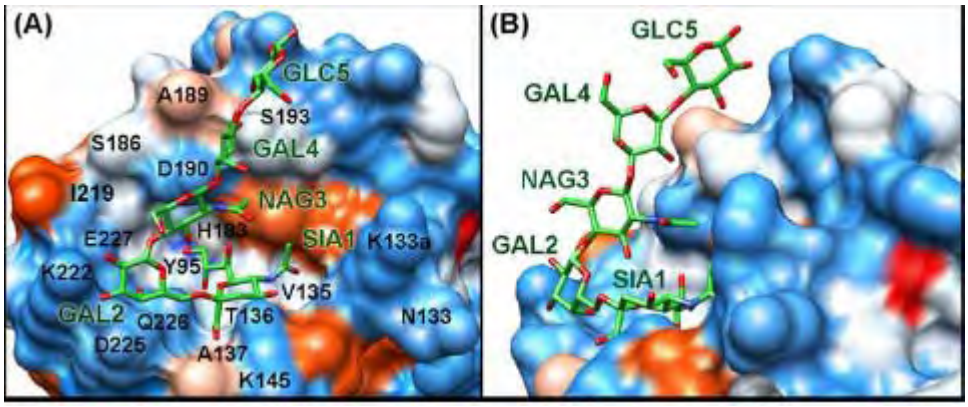

Figure 2 (A) Top and (B) side views of the human SIA-2,6-GAL sialopentasaccharide receptor bound to the binding pocket of the 2009 H1N1 influenza HA. The potentially contact residues and five units of the receptor (SIA1, GAL2, NAG3, GAL4 and GLC5) are labeled. Residue K133a is an inserted amino acid specific to the 2009 H1N1 HA. Blue and orange surfaces indicate the hydrophilic and hydrophobic features, respectively.

Moreover, it is also very interesting to compare the amino acid in receptor binding site of the novel 2009 HA with the previous strains of H1N1 subtypes. The viral genetic sequences in the HA receptor binding domain of the four different H1N1 influenza viruses i.e., the 1918 Spanish flu, 1930 swine flu, 2005 seasonal flu, and 2009 novel flu, are compared and are summarized in Table 1. Using the original 1918 H1N1 HA as the reference, the amino acids at 7 Å spherical radius around the hHAR in the binding pockets of the H1-1930, H1-2005, and H1-2009 HAs contain three (K133aR, T155V and D225G), six (T133N, K133aR, S145N, T155V, A219E and D225G) and seven (T133N, S145K, T155V, P186S, T189A, A219I and A227E) substitutions (shown in bold and underlined in Table 1), respectively. From a

comparison of the hydrophobic plots (Figure 3), the 2009 HA binding pocket displays considerably higher hydrophilic characteristics (represented by the blue surface) than those of the other three HA strains. Since the residues 190 and 225 are known to be a key factor determining the HA-hHAR binding in all H1N1 subtypes,[9, 22-26] and the HAs of all H1N1 strains contain D190, therefore, interest is focused on residue 225 in which G225 was found in the 1930 swine and 2005 seasonal viruses, whereas D225 was detected in the HAs of the two pandemic strains, H1-1918 and H1-2009 (Table 1). In addition, residue A227, which is the receptor binding site that is commonly conserved as "Q226-A227-G228" ("QAG") was replaced by E227 in the novel 2009 influenza virus. Substitution of A227 by the negatively charged E227 residue ("QEG") is supposed to affect the orientation of the surrounding residues.[24] As a consequence, the increase of the hydrophilicity and the replacement of the "QAG" by the "QEG" receptor binding site of the H1-2009 HA are possibly involved in the recognition and familiarity-strength in the binding to the hHAR of the newly emerged flu. **Therefore, in the second part of this work, MD simulations of the hHAR bound to the four HA A/H1N1 influenza viruses were carried out to examine the receptor binding contribution arisen from the differences of electronic and structural properties of the four different HA binding pockets.**

Table 1. Comparison of amino acids in the HA receptor binding domain of the four different H1N1 influenza viruses: the 1918 Spanish flu (H1-1918), 1930 swine flu (H1-1930), 2005 seasonal flu (H1-2005), and 2009 novel flu (H1-2009). Residues are numbered (residue ID) according to 1918 Spanish flu sequence. Using H1-1918 as the reference, the residue differences in the other three isolates are shown in bold and underlined. Residue K133a is an inserted amino acid specific to H1.

	H1N1 HA strains			
Residue ID	H1-1918	H1-1930	H1-2005	H1-2009
95	Y	Y	Y	Y
133	T	T	**N**	**N**
133a	K	**R**	**R**	K
134	G	G	G	G
135	V	V	V	V
136	T	T	T	T
137	A	A	A	A
138	A	A	A	A
145	S	S	**N**	**K**
153	W	W	W	W
155	T	**V**	**V**	**V**
183	H	H	H	H
185	P	P	P	P
186	P	P	P	**S**
189	T	T	T	**A**
190	D	D	D	D
192	Q	Q	Q	Q
193	S	S	S	S
194	L	L	L	L
219	A	A	**E**	**I**

222	K	K	K	K
225	D	**G**	**G**	D
226	Q	Q	Q	Q
227	A	A	A	**E**
228	G	G	G	G

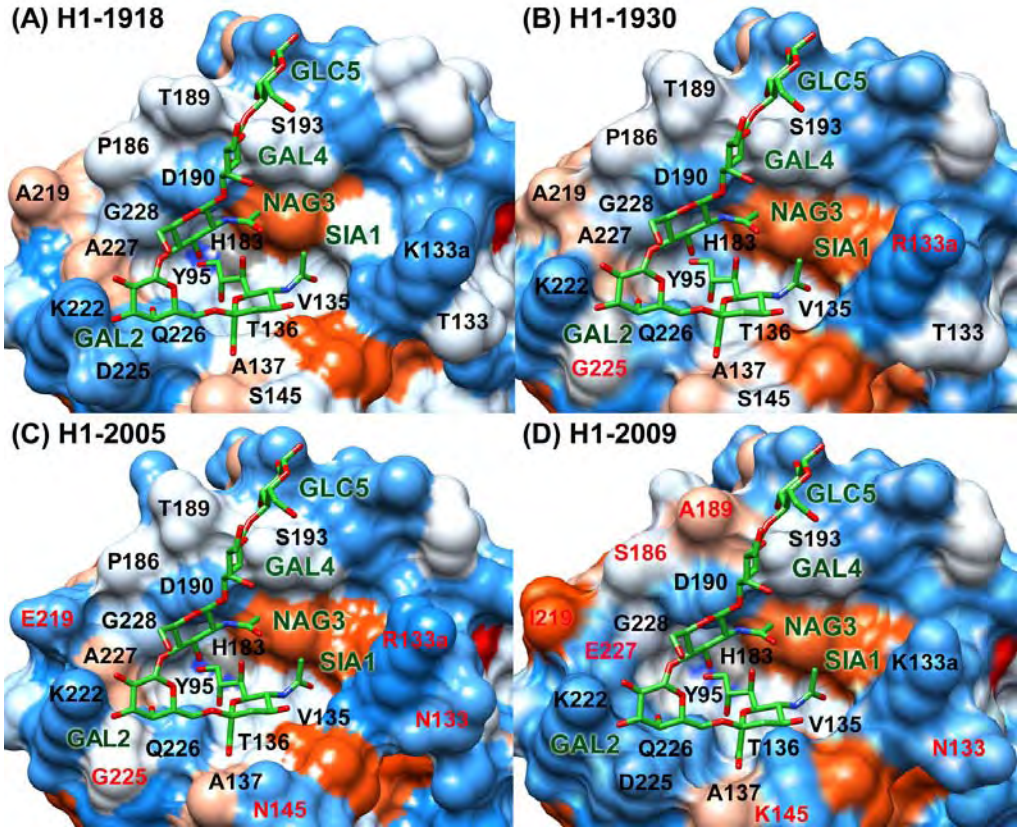

Figure 3. The hHAR in the binding pocket of the four viral influenza A/H1N1 HAs: (A) 1918 Spanish flu (H1-1918), (B) 1930 swine flu (H1-1930), (B) 2005 seasonal flu (H1-2005) and (D) 2009 novel pandemic flu (H1-2009). For H1-1930, H1-2005 and H1-2009, the residues that differ from the reference H1-1918 sequence are shown in red. The hydrophilic and hydrophobic surfaces are colored by blue and orange, respectively.

2. Objectives

The main goals of this research work are:

3.1 To understand how a novel 2009 emerging influenza virus infects human cell

3.2 To compare the HA-hHAR binding efficiency among the four different H1N1 strains of 1918, 1930, 2005, and 2009 HA influenza viruses

3.3 To examine the effects or influences of amino acid changes in receptor binding pocket contributed to HA-hHAR binding efficiency

3. Methodologies

The works are divided into two parts.

3.1 MD simulation of the 2009 HA H1N1 complexed with hHAR

Since there is no experimentally resolved crystal structure of 2009 HA bound with hHAR, the initial structure of the 2009 H1N1 influenza HA complexed with the hHAR was modeled based on the sequence recently isolated from children in Southern California, A/California/04/2009(H1N1) [27]. To search for the most relevant structure of the 2009 HA protein, its amino acid sequence was preliminary aligned to all seven available crystallographic H1N1 HA structures[28]. It was found that the 1930 swine H1N1 HA structure shows the highest amino acid sequence similarity, at 86 % identical (Figure 4). Therefore, the 1930 HA complexed with the hHAR (Protein Data Bank entry code: 1RVT) was chosen as the template [28] for building up the HA-2009 structure by homology modeling technique using the module implemented in the Discovery Studio 2.0[29]. To obtain the 2009 HA-receptor complex, HA protein backbone atoms of 2009 and 1930 isolates were superimposed and coordinates of 1930-HA were removed, retaining only hHAR. The novel H1N1 HA-receptor complex was further refined using energy minimization and followed by the multiple stepwise MD simulations.

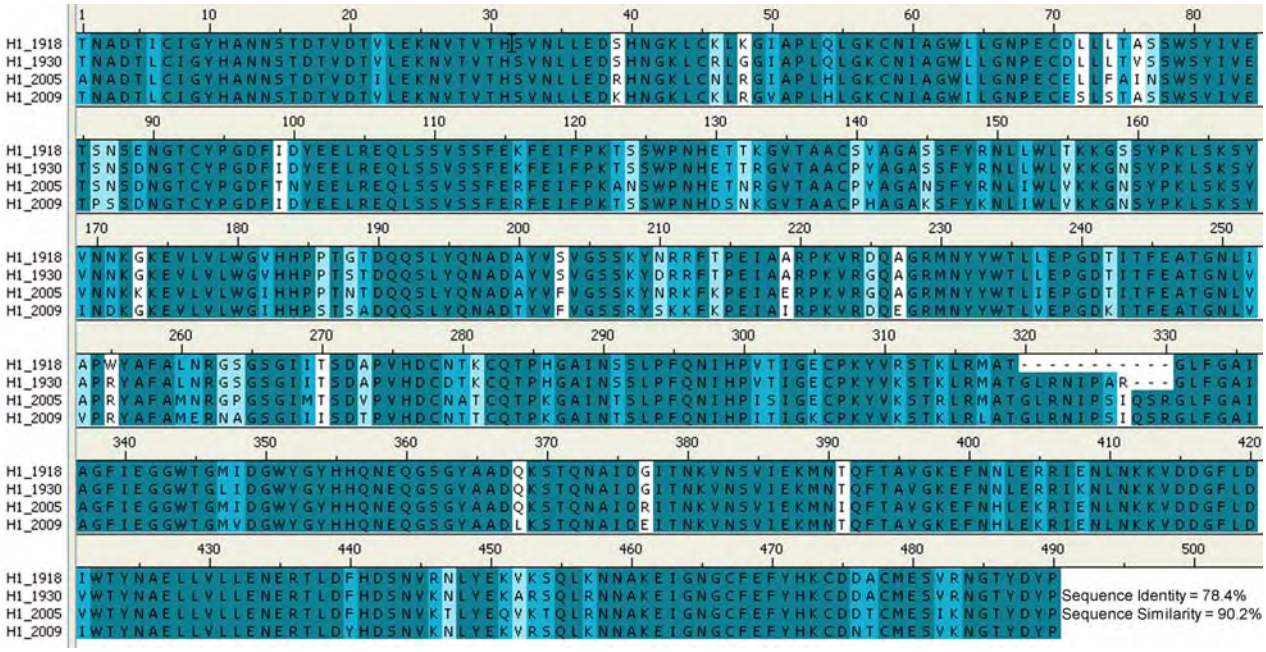

Figure 4 Sequence alignment of a novel 2009 (Accession No. EPI176470), swine 1930, and seasonal 2005 (Accession No. ABY40407) to 1918 H1N1 hemagglutinin influenza A virus.

All simulations of HA-receptor complex were carried out using the SANDER module of the AMBER 10 software package[30]. The HA protein and SIA-α2,6-GAL sialopentasaccharide were parameterized using the AMBER03[31] and the GLYCAM06 force fields[32], respectively. All missing hydrogen atoms were added using the LEaP module[30] and the system was subsequently solvated by a cubic box with dimensions of 66 × 69 × 141 Å filled with TIP3P water molecules. Normal charge states of ionizable amino acids corresponding to pH 7.0 were treated and 5 Cl^- counterions were further added to maintain neutrality on the system. A periodic boundary condition in the isobaric-isothermal (NPT) ensemble with a constant pressure of 1 atm and a temperature of 310 K was set up, whilst a Berendsen coupling time of 0.2 ps was employed to control the temperature. The SHAKE algorithm[33] was applied to constrain all hydrogen bonds using a time step of 2 fs. Non-bonded interactions were calculated with a 12 Å residue-based cutoff and the Particle Mesh Ewald method[34]

was applied to treat the long-range electrostatic interactions. To remove unfavorable contact, the structure of the HA-receptor complexes, was relaxed by performing 3000 steps of conjugated gradient energy minimization. The whole system was subsequently heated from 0 K to 310 K over 100 ps. The system was pre-equilibrated for two steps of 200-ps simulations with position restraints on the receptor atoms with the factors of 80 and 40 $kJ \cdot mol^{-1} \cdot Å^2$, to maintain their coordinates inside the protein binding pocket. Afterwards, the complex was fully simulated for 4 ns.

3.2 Molecular dynamics simulation of the hHAR bound to four different HA strains of H1N1 influenza viruses

The co-crystal structure of the 1930 swine influenza A/H1N1 HA (H1-1930) with the hHAR and the crystal structure of the apo form of the 1918 influenza A/H1N1 HA (H1-1918), were retrieved from the Protein Data Bank (PDB entry codes 1RVT and 1RUZ, respectively),[35] and were used as the starting structures for the MD simulations. To prepare the hHAR bound to the H1-1918 HA, superposition of the H1-1930 and the H1-1918 HA proteins over the backbone carbon atoms was performed and the H1-1930 coordinates were then removed, retaining the coordinates of hHAR. The structure of the 2005 seasonal H1N1 HA complexed with the hHAR was prepared in a similar fashion of the H1-2009.[36] Briefly, using the structure of 1930 swine flu[35] as a template and amino acid sequences of the isolated Influenza A/swine/Chachoengsao/NIAH587/2005(H1N1),[37] the 3D-structure of the 2005 HA protein was created by homology modeling technique using the module implemented in Discovery Studio 2.0.[38] The hHAR bound to the H1-2005 HA was set up in a similar manner to that of the aforementioned H1-1918.

All calculations of the HA-hHAR complexes were carried out using the AMBER 10 software package[30]. The HA proteins and the hHAR were parameterized

using the AMBER03[31] and GLYCAM06 force fields,[32] respectively. Protonation of the ionizable amino acids was assigned at *pH* 7.0 using the PROPKA program.[39, 40] All missing hydrogen atoms were added using the LEaP module implemented in AMBER 10.[30] The simulated system was subsequently solvated by TIP3P water molecules in a cubic box with dimensions of 65 × 68 × 143 $Å^3$ for H1-1918, 65 × 68 × 141 $Å^3$ for H1-1930, and 67 × 68 × 141 $Å^3$ for H1-2005. This is almost comparable to that of 66 × 69 × 141 $Å^3$ used before for the H1-2009 complex.[36] The electroneutrality of the simulated systems was treated by adding 1, 0, 4 and 5 chloride counterions for H1-1918, H1-1930, H1-2005, and H1-2009, respectively. The periodic boundary condition in the isobaric-isothermal (NPT) ensemble with a constant pressure of 1 atm and temperature of 310 K was set up, whereas a Berendsen coupling time of 0.2-ps was employed to control the temperature. Non-bonded interactions were calculated with a 12 Å residue-based cutoff, and the Particle Mesh Ewald method[41] was applied to treat the long-range electrostatic interactions. A 2-fs step size with the SHAKE algorithm[42] was used along the simulations.

The water molecules were first relaxed with 500 steps of steepest descent (SD) and 1,000 steps of conjugated gradient minimizations, while the HA and hHAR coordinates were kept fixed. The whole system was consequently optimized by performing 1,000 steps of SD and 1,000 steps of conjugated gradient minimizations. Afterwards, the systems was heated to 310 K over 100-ps simulation and pre-equilibrated for 400 ps with position restraints on the hHAR atoms with factors of 20 and 10 $kcal \cdot mol^{-1} \cdot Å^{-2}$ to maintain their coordinates inside the receptor-binding pocket. Finally, 6.5-ns simulations were carried out for each HA-hHAR complex and the structural coordinates from the last 5-ns (1.5-6.5-ns) simulations, a production period, were collected for analysis.

4. Results and Discussion

4.1 MD simulation of the 2009 HA H1N1 complexed with hHAR

MD simulation of a novel H1N1 HA complexed with the SIA-2,6-GAL sialopentasaccharide, a human preferential receptor, was carried out over a period of 4 ns. In the last 2.5-ns simulation, the whole system is fairly stable as indicated by the small magnitude of RMSD fluctuation of ca. 0.5 Å (Figure 5). The simulation run could thus provide a suitable basis for the subsequent analyses.

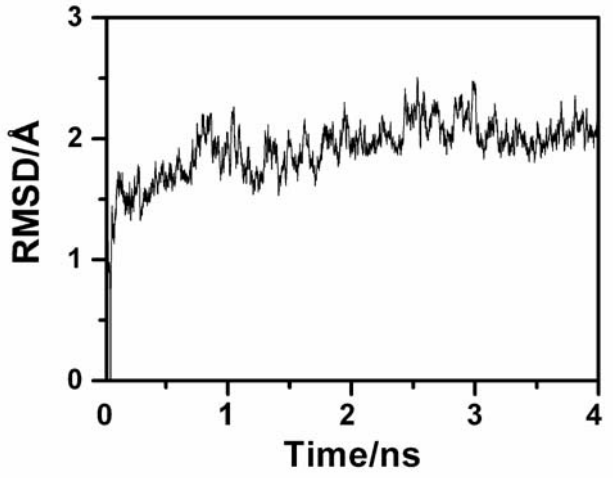

Figure 5 Root-mean-square deviation (RMSD) of all heavy atoms of hemagglutinin and human SIA-α2,6-GAL pentasaccharide receptor to the staring structure as a function of simulation time.

The obtained hHAR was found to properly occupy the binding pocket of the 2009 H1N1 HA, similar to what has been observed experimentally in the other viral influenza HA strains[28, 43-45], where the potentially important contact residues of the 130-loop (K133a, N133, V135, T136 and A137), 190-helix (H183, D190 and S193) and 220-loop (K222, D225, Q226, and E227) as well as Y95 (see Figure 2A for residue positions) were revealed. Structural properties, hydrogen bonds and per residue-receptor interactions are extensively discussed in the following sections.

4.1.1 Sialopentasaccharide receptor conformation

To investigate the conformational character of the human SIA-α2,6-GAL sialopentasaccharide receptor, the distribution of eight important torsion angles, defined in Figure 6A, from *(i)* $\tau 1$-$\tau 4$ bridging between the saccharide units and *(ii)* $\tau 5$-$\tau 8$ of the functional groups of the terminal sialic acid, were measured and plotted in Figures 6B and 6C, respectively.

It can clearly be seen in Figure 6B that the $\tau 1$ and $\tau 2$ torsions of the first three saccharide units (SIA1, GAL2 and NAG3) show a single preferential and sharp peak, suggesting the high stability of these units which were well oriented and occupied in the binding pocket of the enzyme (Figure 2A and 2B) and, therefore, that many hydrogen bonds with the HA residues were firmly formed (Figure 7A, discussed later). The most probable glycosidic torsion angle ($\tau 1$, black line in Figure 6B) was found at ca. -68^{o} indicating the adopted *cis*-conformation of the SIA1 terminal to the GAL2 of the receptor. This proposed conformation is consistent with what has been observed both experimentally and theoretically for the human SIA-α2,6-GAL receptor binding to the influenza HA subtypes H1, H3 and H5 whose glycosidic torsion angles were observed to fall within the range of between -50^{o} and -70^{o}[28, 45-48]. In the same fashion, the $\tau 3$ and $\tau 4$ angles linking between the last three saccharides (NAG3, GAL4 and GLC5) showed the single preferential sharp peak at ca. -73^{o} (Figure 6B) indicating their high rigidity along simulation period.

To reveal the conformational change of the terminal sialic acid, the torsion angles of its functional groups were further evaluated and the results are shown in Figure 6C. Amongst the four angles, $\tau 5$ and $\tau 6$ are slightly broader than the other two

angles, $\tau 7$ and $\tau 8$. This indicates that the -COO- and -NHAc groups could feasibly rotate rather than the hydrophilic group.

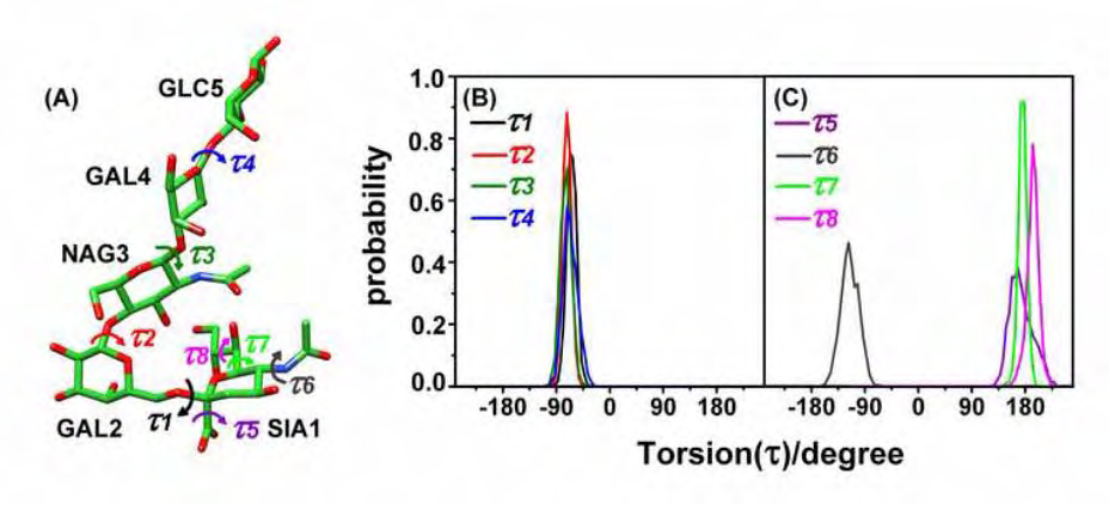

Figure 6 (A) Definition of torsion angles of the human SIA-2,6-GAL sialopentasaccharide receptor. Probability distributions of the (B) torsion angles ($\tau 1$-$\tau 4$) linking between each saccharide unit and (C) torsion angles ($\tau 5$-$\tau 8$) of the functional groups of the terminal sialic acid.

4.1.2 Enzyme-receptor hydrogen bonds

To determine the protein-receptor interactions, hydrogen bonds between the HA residues and the human SIA-α2,6-GAL sialopentasaccharide receptor were calculated according to the two criteria: *(i)* a proton donor (D) and acceptor (A) distance of ≤ 3.5 Å and *(ii)* a D-H..A angle of ≥ 120°.

The number and percentage of hydrogen bond occupation of each of the 2009 HA binding residues and all five saccharides of the receptor were evaluated, and the results are shown in Figure 7A (see description in Table 2). At the terminal sialic acid (SIA1, see Figure 7A), extensive interactions were found with Y95 and the highly conserved residues of the 130-loop (V135, T136 and A137), 190-helix (H183), 220-loop (Q226). The hydroxyl oxygen of the hydrophilic group forms a strong hydrogen

bond to the phenyl group of Y95. Three strong hydrogen bonds were detected between the terminal sialic acid -COO^- group and the three HA residues, T136 and A137 in the 130-loop and Q226 in the 220-loop, whilst the -NHAc moiety established two strong hydrogen bonds with the backbone nitrogen and oxygen atoms of residue V135 in the 130-loop. In addition, the hydroxyl oxygen atoms of hydrophilic side chain form strong and moderate hydrogen bonds with the imidazole ring of H183 in the 190-helix and the amide group of Q226 in the 220-loop, respectively. Based on the numbers of hydrogen bonds (see Figure 7A), the 130-loop is more likely to be in contact with SIA1 than the 190-helix and 220-loop, which is comparable to that of the other hemagglutins complexed with the human receptor[28, 45, 48].

For the second unit of the human SIA-α2,6-GAL sialopentasaccharide receptor (GAL2), two strong hydrogen bonds were formed with the ammonium group of K222 and the backbone oxygen of D225. These hydrogen bonds were also detected in the case of H5 HA-receptor complex, but not in the H3 and H9 HA-receptor complexes [48]. Moreover, two moderate hydrogen bonding interactions between the hydroxyl moieties of this saccharide and the carboxylate group of D225 were also found. Instead, G225, as in the crystal structure of the H1 HA-receptor complex [28, 45], forms hydrogen bonds through its backbone oxygen with the GAL2 unit. Finally, considering the other three units (NAG3, GAL4 and GLC5) of the sialopentasaccharide, they were all found to establish medium to rather weak hydrogen bond networks to the two 190-helix residues, D190 and S193, which are in agreement with the published results of the swine H1-receptor structure [28]. Interestingly, they are, however, different from what has been reported for the H3, H5 and H9 HA-receptor complexes where the last three glycans explicitly interact with the 150-loop and 190-helix.[48]

Taking into account all the simulation results shown above, all the important hydrogen bonds between the SIA-α2,6-GAL sialopentasaccharide receptor and the residues of the 130-loop, 190-helix and 220-loop are considerably conserved and are more likely to be similar to those observed in the H1 HA-receptor complex structure [28, 45], indicating the likely reliability of the simulated structures of the human receptor bound to the pocket of the viral H1N1-2009 HA. In addition, the results also confirm the potentially important role of the 130-loop, 190-helix and 220-loop of the viral surface HA in attaching to SIA-α2,6-GAL sialopentasaccharide glycan, which is the main receptor found in human respiratory tract host cells.

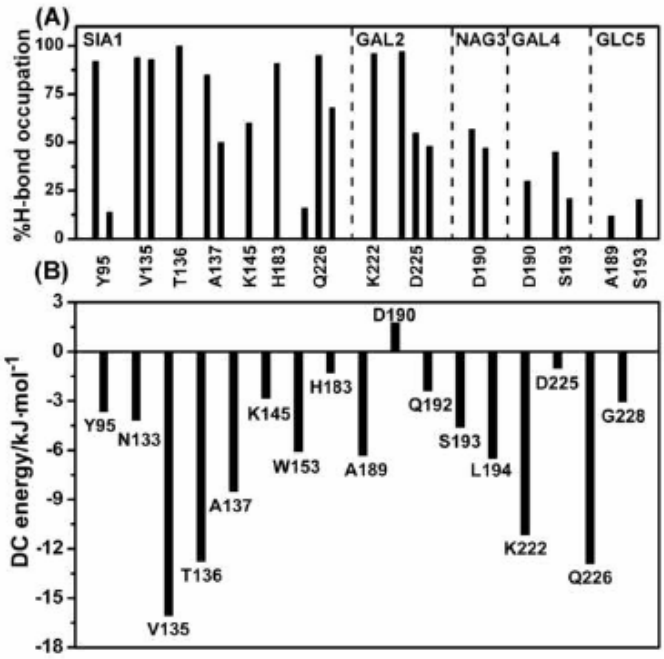

Figure 7 (A) Hydrogen bonding occupation and (B) decomposition (DC) energy in kJ·mol^{-1} of the individual residues of the 2009 H1N1 HA towards the human SIA-2,6-GAL sialopentasaccharide receptor (see Figure 2 for residue labels).

Table 2 Hydrogen bond descriptions and interactions detected between heavy atoms of the human SIA-α2,6-GAL pentasaccharide receptor and 2009-H1N1 hemagglutinin residues.

Pentasaccharide	HA	Type	%Occupation
SIA1	Y95	Y95_OH_H---O8_SIA1	92
	Y95	Y95_OH---H_O9_SIA1	14
	V135	V135_N_H---O5N_SIA1	94
	V135	V135_O---H_N5_SIA1	93
	T136	T136_OG1_H---O1B_SIA1	100
	A137	A137_N_H---O1A_SIA1	85
	A137	A137_N_H---O1B_SIA1	50
	K145	K145_NZ_H---O4_SIA1	60
	H183	H183_NE2---H_O9_SIA1	91
	Q226	Q226_NE2_H---O1A_SIA1	16
	Q226	Q226_NE2_H---O1B_SIA1	95
	Q226	Q226_OE1---H_O8_SIA1	68
GAL2	K222	K222_NZ_H---O3_GAL2	96
	D225	D/G225_O---H_O4_GAL2	97
	D225	D225_OD1---H_O3_GAL2	55
	D225	D225_OD2---H_O3_GAL2	48
NAG3	D190	D190_OD1---H_N2_NAG2	57
	D190	D190_OD2---H_N2_NAG2	47
GAL4	D190	D190_OD1---H_O2_GAL4	30
	S193	S193_OG---H_O2_GAL4	45
	S193	S193_OG_H---O2_GAL4	21
GLC5	A189	T189_O---H_O6_GLC5	12
	S193	S193_OG---H_O3_GLC5	20

4.1.3 Per residue HA enzyme - SIA-α2,6-GAL receptor interactions

To reveal the fundamental basis of the binding between the human SIA-α2,6-GAL sialopentasaccharide receptor and the influenza HA, the interaction energy between each of the individual residues and the SIA-α2,6-GAL sialopentasaccharide were evaluated using the decomposition (DC) energy module, implemented in AMBER 10. The energetic contribution was averaged over a set of 100 MD snapshots, taken at every 25 ps from the last 2.5-ns simulation.

The evaluated DC energies of the HA residues located in the binding pocket were plotted in Figure 7B, where the per residue interaction energies are seen to vary within the range of 2 to -17 kJ·mol^{-1}. The major contribution to the enzyme-receptor interactions was gained from the conserved residues which are the members of the 130- and 220-loops: V135, T136, A137, K222 and Q226. The corresponding DC energies of < -8 kJ·mol^{-1} due to these residues agree well with the hydrogen bond data discussed above (Figure 7A) and corroborates their important role in attaching the viral coat HA to the human SIA-2,6-GAL sialopentasaccharide receptor of susceptible host cells. The higher negative values of the DC data in Figure 7B for the remaining residues of these two loops and the 190-helix residues (except for D190) also indicate their likely responsibilities in stabilizing the human receptor-HA complex. In some contrast, and in agreement with a previous theoretical report, [49] the D190 residue was found to destabilize the protein-receptor complex.

Interestingly, as determined from their DC energies, the D225 and D190 residues do not significantly improve the enzyme-receptor binding affinity, although they interact explicitly via three hydrogen bonds with the GAL2, NAG3 and GAL4 saccharides of the SIA-α2,6-GAL sialopentasaccharide, respectively (as discussed above). This can then be best understood in terms of their total interactions with the neighboring residues, since the DC energy is a summation of all interactions between

a central residue and its environment, including the SIA-α2,6-GAL receptor and all the residues of the respective HA enzyme. In other words, the D225 and D190 hydrogen bond energies can be destabilized by their repulsions with the other residues of the HA.

4.2 Molecular dynamics simulation of the hHAR bound to four different HA strains of H1N1 influenza viruses

4.2.1 Changes of the receptor conformation inside the H1 binding pocket

The attachment of the viral surface homotrimeric glycoprotein HA to the host membrane via the hHAR is believed to be the primary step in the viral replication cycle. To differentiate the receptor's conformation in the binding pocket of the HAs of the Spanish flu (H1-1918), swine flu (H1-1930), seasonal flu (H1-2005) and a novel pandemic flu (H1-2009), the distributions of the torsion angles (τ1-τ9 in Figure 8) were measured and are plotted in Figure 9. As defined in Figure 8, τ1-τ9 were classified in three important regions providing three different characters of the receptor binding, (i) τ1-τ3: conformations of terminal sialic acid (SIA1) α2,6-linked to galactose (GAL2) of the hHAR; (ii) τ4-τ6: orientations of the three side chains of the SIA1 functional groups and (iii) τ7-τ9: bridging between the saccharide units 2 - 5 of the receptor.

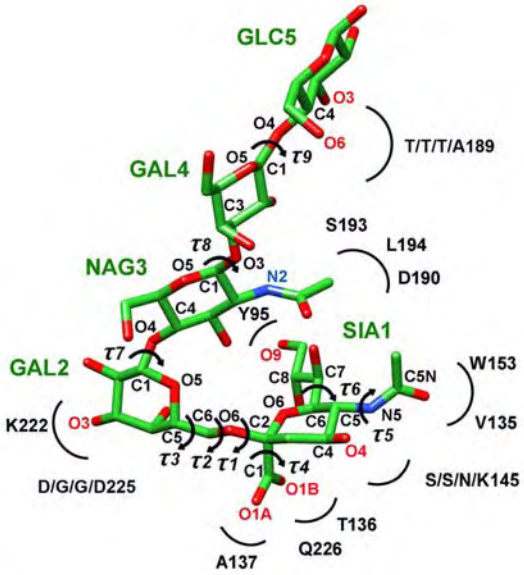

$\tau 1$ = C1 (SIA1) - C2 (SIA1) - O6 (GAL2) - C6 (GAL2)
$\tau 2$ = C2 (SIA1) - O6 (GAL2) - C6 (GAL2) - C5 (GAL2)
$\tau 3$ = O6 (GAL2) - C6 (GAL2) - C5 (GAL2) - O5 (GAI2)
$\tau 4$ = O1A (SIA1) - C1 (SIA1) - C2 (SIA1) - O6 (SIA1)
$\tau 5$ = C4 (SIA1) - C5 (SIA1) - N5 (SIA1) - C5N (SIA1)
$\tau 6$ = C5 (SIA1) - C6 (SIA1) - C7 (SIA1) - C8 (SIA1)
$\tau 7$ = O5 (GAL2) - C1 (GAL2) - O4 (NAG3) - C4 (NAG3)
$\tau 8$ = O5 (NAG3) - C1 (NAG3) - O3 (GAL4) - C3 (GAL4)
$\tau 9$ = O5 (GAL4) - C1 (GAI4) - O4 (GLC5) - C4 (GLC5)

Figure 8 Schematic representation and definitions of the τ1-τ9 torsion angles of the hHAR in the binding site of the HA subtype H1. Some labeled atoms used in the results and discussion are also shown. The labels, such as S/S/N/K145, were used to represent the four different amino acids in the same sequence number of the 1918-, 1930-, 2005- and 2009-H1N1 HAs, respectively.

The distributions of the torsion angle plots (Figure 9), excluding τ9 of H1-1930 and τ4 of H1-2005, reveal clearly that all torsion angles of the four HA-hHAR systems show a sharp peak at almost the same position, suggesting that the hHAR adapts itself very well to reach its optimal structure within the four H1NI HA binding sites.

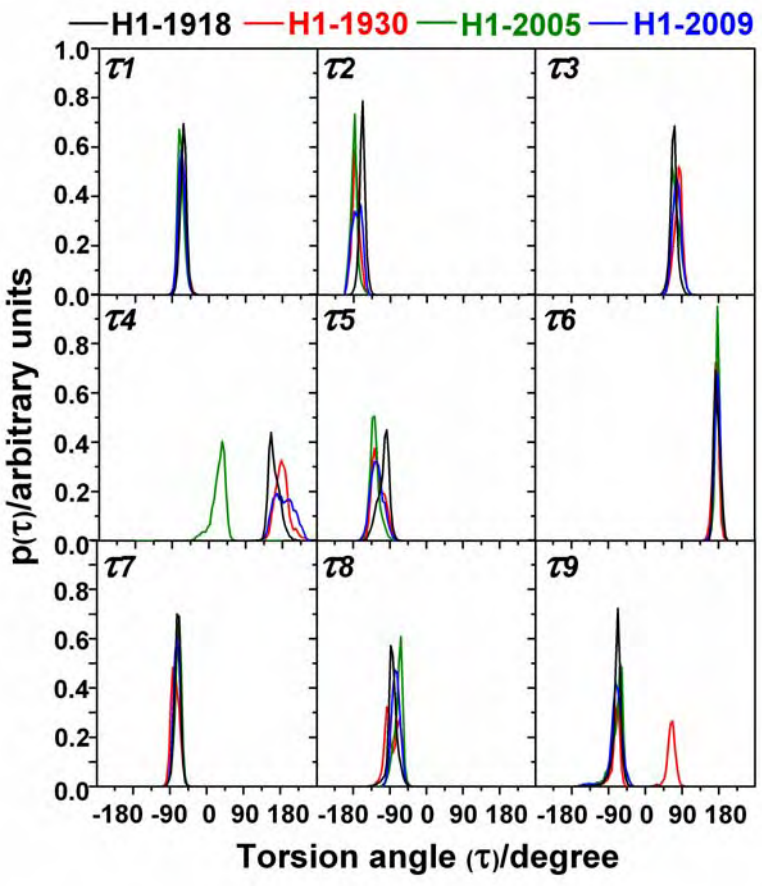

Figure 9 Distribution plots of the torsion angles (τ1-τ9) of the hHAR lying within the binding pocket of the HA of the four H1N1 strains (H1-1918, H1-1930, H1-2005 and H1-2009).

The τ1-τ3 angles on the single bonds linking between the six-membered rings of the SIA1 terminus and the GAL2 unit show a sharp peak at ca. -65°, -165° and 70°, respectively, indicating an identical orientation of these two sugars puckered into the HA pocket site. The τ1 glycosidic torsion of ca. -65° represents their cis-conformation on the α-ketosidic linkage corresponding to those commonly observed in the SIA-α2,6-GAL receptor (hHAR) bound to other HAs by both experimental and theoretical studies.[35, 50-53] Considering the orientations of the three side chains of the SIA1, the difference was only found at the carboxylate group of the H1-2005 in which its τ4 was detected at ca. 30° relative to ca. 180° for the other HAs, i.e., in difference from

the other systems, the O1A group (see Figure 8) of the H1-2005 was rotated into the binding site to interact with the HA residues. The τ6 angle of the hydrophilic moiety displayed a sharper peak than the τ4 of the –COO- and τ5 of the –NHAc groups, indicating that these two side chains are slightly more flexible in a narrow range in comparison with the hydrophilic group of the terminal SIA1.

For the remaining sugar moieties lying on the surface-exposed region of the hHAR protein (see Figure 3), the structural conformations of the NAG3 and GAL4 were found to be similar among the four HAs, as presented by the same degrees of τ7 and τ8 angles (-70° and -80°, respectively, in Figure 8). However, the orientation of the last glycan unit, GLC5, in the H1-1930 (τ9 of 65°, red line) was somewhat different from the other three HAs (τ9 of -65°). Therefore, different intermolecular interactions of the terminal GLC5 sugar of the saccharide chain with the protein surface residues are to be expected in the H1-1930 case (details in the following sections).

4.2.2 Enzyme-receptor interactions

To gain insight into the efficiency of the hHAR binding to the HAs of H1-1918, H1-1930, H1-2005, and H1-2009, the percentage and number of hydrogen bonds between this receptor and the contact residues of HAs were measured according to the subsequent criteria: (i) the distance between proton donor (D) and acceptor (A) atoms ≤ 3.5 Å; and (ii) the D-H…A angle ≥ 120°. The results are shown in Figure 9 and the hydrogen bond descriptions are given in Table 3.

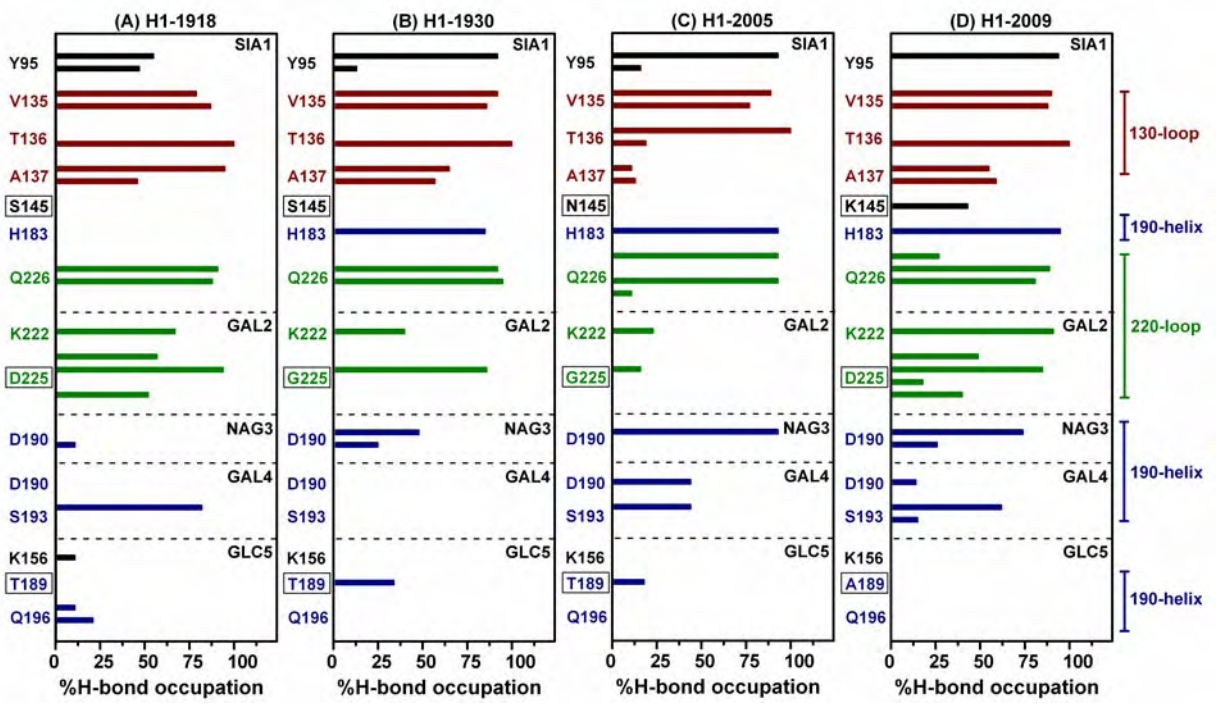

Figure 9 Hydrogen bond occupation between the five saccharide units (SIA1, GAL2, NAG3, GAL4 and GLC5) of the hHAR and the HA binding residues of (A) Spanish flu (H1-1918), (B) swine flu (H1-1930), (C) seasonal flu (H1-2005) and (D) a novel flu (H1-2009). The residues which are different among the four HAs are shown with a box around the label (see Figure 3 for residue positions). Residues of the 130-loop, 190-helix and 220-loops are colored by red, blue and green, respectively.

As shown in Figure 9, hydrogen bonds between the hHAR and the HA residues in all systems can be firmly formed in the three important binding HA regions: 130-loop, 190-helix and 220-loop, especially at the sialic acid terminus which is inserted directly into the receptor-binding pocket of the HA. Strong hydrogen bonds are almost conserved at the residues Y95, V135, T136, A137, and Q226 of the four HA strains. Note that major interactions between the SIA1 and the T136 and Q226 are maintained although different hydrogen bonding pattern was detected, i.e., the interaction takes place via the O1A in the H1-2005 and the O1B in the other HAs. Noticeably change was found when the S/S/N145 – a polar residue with non-charged

side chain – in the H1-1918, H1-1930, and H1-2005 was replaced by the K145 – a positively charged residue in a novel HA. This makes the H1-2009 capable of establishing one moderate hydrogen bond to the O4 of SIA1. The observed results lead to conclusion that introducing of the fourth lysine (K145) of the lysine fence (K133, K156, and K222) in the HA of the 2009 facilitates stronger enzyme-receptor binding by better anchoring the SIA1 terminus. This observation is in agreement with the recently proposed hypothesis.[54] Furthermore, a strong hydrogen bond between the H183 and the O9 of SIA1 was observed in the H1-1930, H1-2005 and H1-2009 complexes whereas this kind of interaction was disappeared in the case of H1-1918 system.

A major difference was additionally found at the connecting GAL2 unit, where the number and percentage of hydrogen bonding interactions detected at the HA 220-loop on residues K222 and D/G/G/D225 are much stronger for H1-1918 and H1-2009 than those of H1-1930 and H1-2005 (Figure 9). It is clear that for the D/G/G/D225 binding, the direct electrostatic effects, due to the negatively charged D225 residue, lead to a more effective interaction in the H1-1918 and the H1-2009 viral HAs than the non-charged G225 in the HA of the H1-1930 and H1-2005 viruses. For the K222-GAL2 binding, the moderate and strong hydrogen bonds between O3 of this particular unit and the K222 residue in the HA of H1-1918 and H1-2009 were observed. This is possibly affected by the indirect effects due to the presence of one (D225) and two (D225 and E227) negatively charged residues in the binding pocket of H1-1918 and H1-2009, respectively. In 2009 influenza pandemic strain, the orientation of the K222 residue was mainly stabilized by both D225 and E227 residues through electrostatic and salt-bridge interactions, respectively (see Figure 10D and more discussion in the next section) whereas only D225 was observed to stabilize K222 in the case of H1-1918. This is in contrast with what was found for the

H1-1930 and H1-2005 viruses, where both the G225 and A227 residues are hydrophobic, leading to a lowering of the electrostatic potential in this region, relative to those of the other two systems. This provides a clear reason why K222 could not form a stable hydrogen bond with GAL2 in the H1-1930 and H1-2005 HAs (Figures 9B and 9C, respectively). This hypothesis is further analyzed in terms of the electrostatic potential plot in the next section. A crucial role of residue 225 has been reported previously,[9, 23, 24] with the additional hypothesis that mutation of this residue could result in a reduced viral binding affinity to the hHAR. It has also been experimentally found that the presence of the G225 residue in the HA of H1-1930 and H1-2005 apparently reduced the binding efficiency of the virus to the hHAR.[4, 9, 24]

With respect to the NAG3, GAL4 and GLC5 saccharide units, which lay on the surface exposed region (Figure 3), far from the binding pocket, and are supposed to play only a minor role in holding the receptor in place, a lower percentage and number of hydrogen bonds were found (Figure 9) in comparison to those observed at the first two units (SIA1 and GAL2) of the receptor. Their interactions were moderately strong with 190-helix residues T/T/T/A189, D190, and S193.

Taking into account all the above given data, the order of hydrogen bond strengths of the hHAR binding to the H1N1 HAs was H1-2009 > H1-1918 > H1-2005 ≅ H1-1930. The increase of binding affinity in the novel H1-2009 (H1N1) HA to the hHAR is mainly due to the higher hydrophilicity at the receptor binding domain, in which residues 145, 225 and 227 were found to play a critical role. The transmissibility of the 2009 H1N1 virus (depending upon several external factors and determined by the basic reproduction number, R_0 of 1.2 - 1.6) falls within the range of the 1918 Spanish flu (R_0 of 1.4 - 2.8) but is higher than that of seasonal influenza virus (R_0 of 0.9 - 2.1).[55, 56] This transmission ability is supposed to relate, somewhat, to the predicted enzyme-receptor binding affinity. Note that the pathogenesis and

transmission studies of the 2009 H1N1 influenza virus indicated that a novel flu was observed to be more pathogenic than the seasonal H1N1 virus.[56, 57] Since the 2009 influenza virus could deeply penetrate into the airways and exhibits more extensive viral replication in the respiratory tract, its severity could potentially increase in comparison with seasonal virus.[56, 57]

4.2.3 Effect of charged residues on the receptor binding affinity

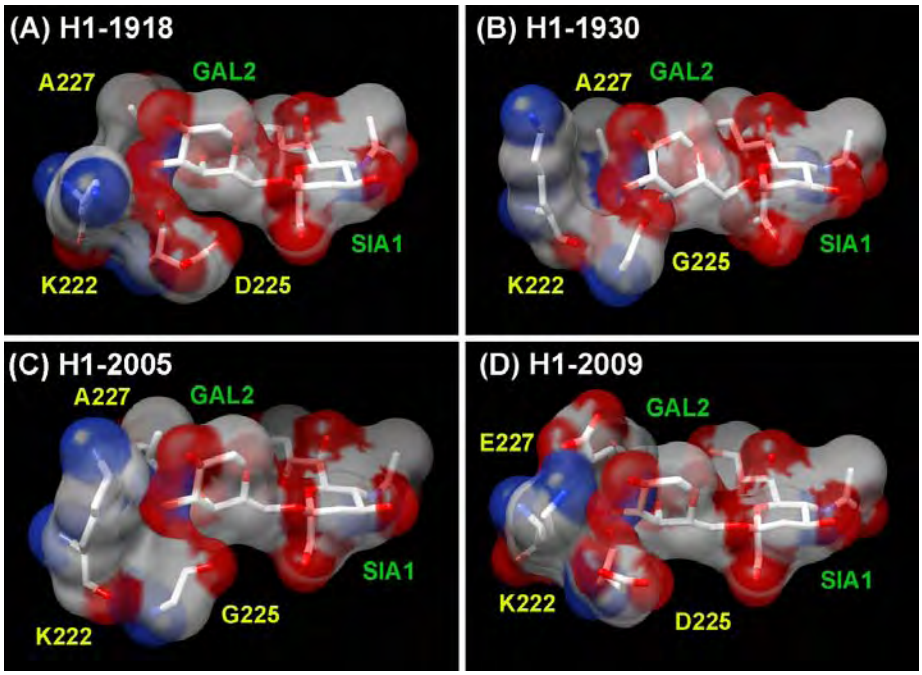

Figure 10 Electrostatic potential map of hHAR and HA binding residues K222, D/G/G/D225 and A/A/A/E227 of (A) Spanish flu (H1-1918), (B) swine flu (H1-1930), (C) seasonal flu (H1-2005) and (D) novel flu (H1-2009). Positive and negative electrostatic potentials are represented by blue and red, respectively.

As already mentioned, hydrogen bond analysis revealed that introduction of charged amino acids in the receptor binding domain of the novel HA influenza virus could effectively contribute to the binding with the hHAR, in particular HA residues 222, 225 and 227. Therefore, to provide an additional perspective on the contribution of the polar residues to the hHAR-HA binding, the electrostatic isosurface maps of the

hHAR and the HA 222, 225 and 227 residues were plotted in Figure 10. The positive and negative electrostatic potentials are indicated by blue and red, respectively.

In all systems, the negative electrostatic potentials (Figure 10, red) were found around the SIA1 and GAL2 units of the hHAR, while a positive electrostatic potential was generated over the K222 residue (Figure 10, blue). Differences between the four viral HAs are clearly and obviously observed in the region around the 225 and 227 residues. Here, changing the negatively charged D225 residue in the 1918- and 2009-H1N1 models to a non-polar G225 residue (Table 2) leads to the negative electrostatic potential around residue 225 almost totally disappearing (the red regions in Figures 10A and 10D change to white in Figures 10B and 10C, respectively). In addition, the substitution of a non-polar A227 residue of the 1918-, 1930- and 2005-H1N1 HAs (Table 2) with a negatively charged E227 residue in the HA of H1-2009 leads additionally to an enhanced negative electrostatic potential around the 227 residue (the red region, which is only observed in Figure 10D).

As a consequence, the electrostatically negative potentials near residues D225 and E227 are unique in the H1-2009 H1N1 isolate (of the four studied) and the enhanced electronegative isosurface could potentially stabilize the ionic network of the 220-loop residues K222, D225 and E227. This helps the K222 residue to adjust its conformation to be in optimal contact with the GAL2 moiety of the hHAR, leading to the formation of a strong hydrogen bond in the H1-2009 HA–hHAR complex (Figure 4D), as previously discussed. On the other hand, the electrostatic potentials that result from the combination of the charged- and non-charged residues (D225 and A227) can potentially induce the moderate K222-GAL2 hydrogen bond formation in the H1-1918 HA-hHAR interaction (Figure 10A). This is not the case for the H1-1930 and H1-2005 HAs (Figures 9B and 9C, respectively), where this hydrogen bond is very

weak because both G225 and A227 are fully uncharged and could not establish such ionic network with the K222.

4.2.4 Role of the non-conserved residue 227

Although residue 227 was found to vary between the influenza A viral strains, the receptor binding residues Q226 and G228 are highly conserved, forming a "Q226-X227-G228" pattern or so called "QXG" site, where QSG and QGG sites are found in the avian H3 or H5 and H2 influenza virus HAs, respectively.[24, 58] In this study, both the 1918-, 1930-, and 2005-H1N1 strains contain the QAG sequences, whereas the 2009-novel flu (H1-2009) shows a unique QEG site. The increased hydrophilicity in the receptor binding region is apparently the development of the current pandemic flu from the 1918 Spanish, the 1930 swine and the seasonal 2005 flues. As shown and described in the previous sections, substitution of the non-charged A227 residue with the negatively charged E227 improves the binding of HA to the hHAR and this is potentially attained by establishing the ionic network with the K222 and D225 residues. This finding thus indicates that the non-conserved residue 227 possibly plays a critical role in the evolution of a new and potentially more pathogenic H1N1 influenza virus. Note that among the three residues in the HA "QXG" site of the four H1 strains under this study, Q226 is the only residue that interacts directly with the hHAR via strong hydrogen bonds (Figure 9).

4.2.5 Human HAR solvation

Solvation of the hHAR was monitored in terms of atom-atom radial distribution functions, RDFs, gxy(r)—the probability of finding a particle of type y within a sphere radius r around the particle of type x. The RDFs from all heteroatoms of the hHAR to the oxygen atom of water were evaluated. The selected RDFs and the corresponding running coordination numbers, n(r), are shown in Figure 11.

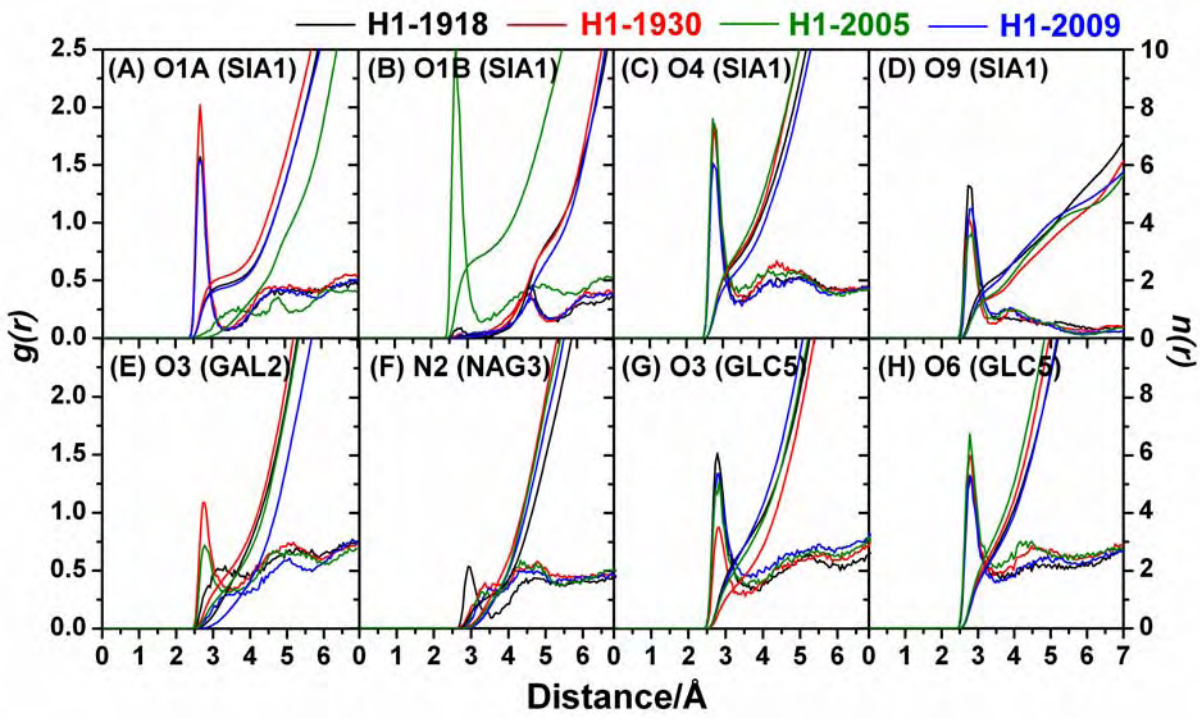

Figure 11 Radial distribution function, g(r), centered on the selected heteroatoms of the hHAR (see Figure 2 for atomic labels) to oxygen atoms of water molecules and the running coordination number, n(r), for the four simulated HA–hHAR systems.

For all HA–hHAR complexes, the major differences in the g(r) at the SIA1 terminus takes place only on the O1B atom (see Figure 3 for atomic label), where the plot for the H1-2005 complex shows the first sharp peak at ~2.7 Å with the corresponding coordination number n(r) integrated up to its first minimum of 2.8 water molecules (Figure 11B, right axis). This indicates that the water was firmly coordinated to the O1B atom of the H1-2005, but not in the HA-hHAR systems of H1-1918, H1-1930 and H1-2009. This is because of the interchange of the O1A and O1B positions due to the rotation of the τ4 angle (see Figure 11).

Although no significant difference was found in terms of the peak position of the RDFs of the other atoms of the SIA1 (Figures 11A, 11C and 11D), however, the n(r) of the H1-1918, H1-1930 and H1-2005 show a higher average number of water

molecules located around this glycan unit than that detected in the H1-2009. In other words, the SIA1 of the hHAR in the HA-hHAR complex of the H1-2009 virus is less solvated than that with the other three HAs. This is consistent with the hydrogen bond data (Figure 9), where a greater level of direct contact leads to the formation of more hHAR-HA hydrogen bonds with the H1-2009 than with the other three viral strains. A clear example is the moderate hydrogen bonding between the O4 atom of SIA1 of the hHAR and the guanidinium group of the HA K145 residue that only takes place in H1-2009 (Figure 9D). Another example that supports the degree of the solvation of O9 atom (Figure 11D) is the strong hydrogen bonding between this oxygen and the HA H183 residue, which is in a reverse order of the first shell coordination numbers for O9 of 1.5 1.5, 2.0 and 2.5 water molecules for H1-2005, H1-1930, H1-2009 and H1-1918, respectively.

For the other four glycan units, the following significant differences were found; O3 of GAL2 (Figure 11E), N2 of NAG3 (Figure 11F) and O3 of GLC5 (Figure 11G) in which the degree of solvation also supports the hydrogen bond data discussed previously (Figure 9).

5. Conclusion

In this research work, three dimensional structure of the hHAR receptor bound to the recently detected 2009 H1N1 HA was modeled based on a homology modeling approach and consequently performed by MD simulations. In comparison to the other influenza HA-hHAR complexes, the simulated results of this receptor binding to the 2009 H1N1 influenza HA provided the highest similarity to those from the structure of the H1-receptor complex. This is mainly due to the fact that they belong to the identical HA subtype and so are likely to share the highest conformational as well as primary sequence similarity. Although many experimental aspects of the 2009 H1N1

outbreak, including its virulence and pandemic potential are still uncertain, our molecular information could provide a better understanding in the first step of the viral life cycle based on how the viral surface glycoprotein HA of the 2009 influenza A (H1N1) efficiently attaches and tightly binds with the hHAR.

In addition, MD simulations of the hHAR bound to the four different HAs of the 1918-, 1930, 2005- and 2009-H1N1 influenza viruses were also studied and compared. We found that the crucial presence of a positively charged K145 residue in the HA of the novel H1-2009 can potentially make a lysine fence with residues K133, K156 and K222 and provides an optimal contact to hydrogen bond with the SIA1 of the hHAR. Owing to the presence of an uncharged S/S/N145 residue in place of the K145, such an ionic network was not created in the Spanish 1918, swine 1930 or seasonal 2005 virions, resulting in the lower potency of HA-hHAR binding. As observed in the all H1N1 strains,[22, 24, 26] HA residue 225 plays a critical role in the hHAR GAL2 binding efficiency. The presence of a negatively charged D225 residue in the HAs of the H1-1918 and H1-2009 could provide a larger number of hydrogen bonds in the HA–hHAR complex than that observed in H1-1930 and H1-2005, where a non-charged G225 residue exists instead. Q226 of the “QAG” (1918-, 1930- and 2005-H1N1) or “QEG” (2009-H1N1) HA sequence directly interacts with the hHAR SIA1 terminus via hydrogen bonds, while the non-conserved 227 residue was found to play a role in stabilizing the enzyme structure around the K222 residue. Introduction of the negatively charged HA E227 residue in the H1-2009 substantially enhanced the HA-hHAR binding efficiency through hydrogen bonds formation between the HA K222 residue and the GAL2 unit of the hHAR. The efficiency of the hHAR binding to the HA of the novel 2009 H1N1 viral strain is greater than that in the 1918 Spanish and the 2005 seasonal (which is comparable to the 1930 swine) influenza viruses, respectively. A major contribution to the virion HA–cellular hHAR binding in H1-

2009 is apparently gained from the charged residues existing in the HA binding pocket. Our simulated results provide a better understanding of how the viral surface glycoprotein HA of different H1N1 strains efficiently attach and bind to the hHAR.

6. Suggestions for future works:

Although many HA studies have been carried out, there are still many open questions concerning this particular glycoprotein and it would very interesting to:

A) Search for active inhibitors against HA protein, in particular at the receptor binding region and membrane fusion

B) Simulate the HA-inhibitor complex. This would be useful to future development of potent HA drugs.

C) Investigate the mechanism or function of HA by using high accuracy method

D) Extend MD simulations for longer time period to see whether dynamical behaviors of protein-receptor complexes are significantly different from that reported in this work

References

1. http://www.who.int/csr/disease/swineflu/en/index.html.

2. http://www.cdc.gov/h1n1flu/.

3. Neumann, G.; Noda, T.; Kawaoka, Y., Emergence and pandemic potential of swine-origin H1N1 influenza virus. *Nature* **2009,** 459, 931-939.

4. Shen, J.; Ma, J.; Wang, Q., Evolutionary Trends of A(H1N1) Influenza Virus Hemagglutinin Since 1918. *PLoS One* **2009,** 4, e7789 doi:10.1371/ journal. pone. 000778.

5. Krug, R. M.; Aramini, J. M., Emerging antiviral targets for influenza A virus. *Trends Pharmacol Sci.* **2009,** 30, 269-277.

6. Steinhauer, D. A., Role of hemagglutinin cleavage for the pathogenicity of influenza virus. *Virology* **1999,** 258, 1-20.

7. Horimoto, T.; Kawaoka, Y., Pandemic threat posed by avian influenza A viruses. *Clin. Microbiol. Rev* **2001**, 129-141.

8. Cross, K. J.; Burleigh, L. M.; Steinhauer, D., Mechanisms of cell entry by influenza virus. *Expert. Rev. Mol. Med* **2001,** 6, 1-18.

9. Stevens, J.; Blixt, O.; Tumpey, T. M.; Taubenberger, J. K.; Paulson, J. C.; Wilson, I. A., Structure and receptor specificity of the hemagglutinin from an H5N1 influenza virus. *Science* **2006,** 312, 404-410.

10. Wiley, D. C.; Skehel, J. J., The structure and function of the hemagglutinin membrane glycoprotein of influenza virus. *Annu. Rev. Biochem.* **1987,** 56, 365-394.

11. Skehel, J. J.; Wiley, D. C., Receptor binding and membrane fusion in virus entry: the influenza hemagglutinin. *Ann. Rev. Biochem.* **2000,** 69, 531-569.

12. Chandrasekaran, A.; Srinivasan, A.; Raman, R.; Viswanathan, K.; Raguram, S.; Tumpey, T. M.; Sasisekharan, V.; Sasisekharan, R., Glycan topology determines

human adaptation of avian H5N1 virus hemagglutinin. *Nat. Biotechnol.* **2008,** 26, 107-113.

13. Bateman, A. C.; Busch, M. G.; Karasin, A. I.; Bovin, N.; Olsen, C. W., Amino acid 226 in the hemagglutinin of H4N6 influenza virus determines binding affinity for alpha-2,6-linked sialic acid and infectivity levels in primary swine and human respiratory epithelial cells. *J. Virol.* **2008,** 82, 8204-8209.

14. Gambaryan, A. S.; Karasin, A. I.; Tuzikov, A. B.; A.A. Chinarev; Pazynina, G. V.; Bovin, N. V.; Matrosovich, M. N.; Olsen, C. W.; Klimov, A. I., Receptor-binding properties of swine influenza viruses isolated and propagated in MDCK cells. *Virus. Res.* **2005,** 114, 15-22.

15. Matrosovich, M. N.; Gambaryan, A. S.; Teneberg, S.; Piskarev, V. E.; Yamnikova, S. S.; Lvov, D. K.; Robertson, J. S.; Karlsson, K. A., Avian influenza a viruses differ from human viruses by recognition of sialyloligosaccharides and gangliosides and by a higher conservation of the HA receptor-binding site. *Virology* **1997,** 233, 224-234.

16. Rogers, G. N.; D⁄Souza, B. L., Receptor binding properties of human and animal H1 influenza virus isolates. *Virology* **1989,** 173, 317-322.

17. Suzuki, Y.; Ito, T.; Suzuki, T.; Holl, R. E.; Chambers, T. M.; Kiso, M.; Ishida, H.; Kawaoka, Y., Sialic acid species as a determinant of the host range of influenza A viruses. *J. Virol.* **2000,** 74, 11825-11831.

18. Russell, R. J.; Stevens, D. J.; Haire, L. F.; Gamblin, S. J.; Skehel, J. J., Avian and human receptor binding by hemagglutinins of influenza A viruses. *Glycoconjugate. J.* **2006,** 23, 85-92.

19. Riel, D.; Munster, V. J.; de Wit, E.; Rimmelzwaan, G. F.; Fouchier, R. A. M.; Osterhaus, A.; Kuiken, T., Human and avian influenza viruses target different cells in

the lower respiratory tract of humans and other mammals. *Am. J. Pathol.* **2007,** 171, 1215-1223.

20. Nicholls, J. M.; Bourne, A. J.; Chen, H.; Guan, Y.; Peiris, J. S. M., Sialic acid receptor detection in the human respiratory tract: evidence for widespread distribution of potential binding sites for human and avian influenza viruses. *Respir Res.* **2007,** 8, 73-82.

21. Soundararajan, V.; Tharakaraman, K.; Raman, R.; Raguram, S.; Shriver, Z.; Sasisekharan, V.; Sasisekharan, R., Extrapolating from sequence-the 2009 H1N1 〝swine〞 influenza virus. *Nat. Biotechnol.* **2009,** 27, 510-313.

22. Glaser, L.; Stevens, J.; Zamarin, D.; Wilson, I. A.; Garcı´a-Sastre, A.; Tumpey, T. M.; Basler, C. F.; Taubenberger, J. K.; Palese, P., A Single Amino Acid Substitution in 1918 Influenza Virus Hemagglutinin Changes Receptor Binding Specificity. *J. Virol.* **2005,** 79, 11533-11536.

23. Taubenberger, J. K., Influenza hemagglutinin attachment to target cells: 〝birds do it, we do it〞. *Future Virol.* **2006,** 1, 415-418.

24. Matrosovich, M.; Tuzikov, A.; Bovin, N.; Gambaryan, A.; Klimov, A.; Castrucci, M. R.; Donatelli, I.; Kawaoka, Y., Early Alterations of the Receptor-Binding Properties of H1, H2, and H3 Avian Influenza Virus Hemagglutinins after Their Introduction into Mammals. *J. Virol.* **2000,** 74, 8502-8512.

25. Yang, Z.-Y.; Wei, C.J.; Kong, W. P.; Wu, L.; Xu, L.; Smith, D. F.; Nabel, G. J., Immunization by Avian H5 Influenza Hemagglutinin Mutants with Altered Receptor Binding Specificity. *Science.* **2007,** 317, 825-828.

26. Stevens, J.; Blixt, O.; Glaser, L.; Taubenberger, J. K.; Palese, P.; Paulson, J. C.; Wilson, I. A., Glycan microarray analysis of the hemagglutinins from modern and

pandemic influenza viruses reveals different receptor specificities. *J. Mol. Biol.* **2006,** 355, 1143-1155.

27. http://www.ncbi.nlm.nih.gov/genomes/FLU/SwineFlu.html.

28. Gamblin, S. J.; Haire, L. F.; Russell, R. J.; Stevens, D. J.; Xiao, B.; Ha, Y.; Vasisht, N.; Steinhauer, D. A.; Daniels, R. S.; Elliot, A.; Wiley, D. C.; Skehel, J. J., The structure and receptor binding properties of the 1918 influenza hemagglutinin. *Science* **2004,** 303, 1838-1842.

29. Discovery Studio 2.0, A. I., San Diego, CA, USA.

30. Case, D. A.; Darden, T. A.; CheathamIII, T. E.; Simmerling, C. L.; Wang, J.; Duke, R. E.; Luo, R.; Crowley, M.; Walker, R. C.; Zhang, W.; Merz, K. M.; Wang, B.; Hayik, S.; Roitberg, A.; Seabra, G.; Kolossváry, I.; Wong, K. F.; Paesani, F.; Vanicek, J.; Wu, X.; Brozell, S. R.; Steinbrecher, T.; Gohlke, H.; Yang, L.; Tan, C.; Mongan, J.; Hornak, V.; Mathews, G. C. D. H.; Seetin, M. G.; Sagui, C.; Babin, V.; Kollman, P. A. *AMBER10*, University of California, San Francisco: 2008.

31. Duan, Y.; Wu, C.; Chowdhury, S.; Lee, M. C.; Xiong, G.; Zhang, W.; Yang, R.; Cieplak, P.; Luo, R.; Lee, T.; Caldwell, J.; Wang, J.; Kollman, P., A Point-Charge Force field for Molecular Mechanics Simulations of Proteins Based on Condensed-Phase Quantum Mechanical Calculations. *J. Comput. Chem.* **2003,** 24, 1999-2012.

32. Tessier, M. B.; Demarco, M. L.; Yongye, A. B.; Woods, R. J., Extension of the GLYCAM06 biomolecular force field to lipids, lipid bilayers and glycolipids. *Mol. Simulat.* **2008,** 34, 349-364.

33. Ryckaert, J. P.; Ciccotti, G.; Berendsen, H. J. C., Numerical integration of the cartesian equations of motion of a system with constraints: molecular dynamics of n-alkanes. *J. Comput. Phys* **1997,** 23, 327-341.

34. Darden, T.; York, D.; Pedersen, L., Particle mesh Ewald: an N–log(N) method for Ewald sums in large systems. *J. Chem. Phys.* **1993,** 98, 10089–10092.

35. Gamblin, S. J.; Haire, L. F.; Russell, R. J.; Stevens, D. J.; Xiao, B.; Ha, Y.; Vasisht, N.; Steinhauer, D. A.; Daniels, R. S.; Elliot, A.; Wiley, D. C.; Skehel, J. J., The Structure and Receptor-Binding Properties of the 1918 Influenza Hemagglutinin. *Science* **2004,** 303, 1838-1842.

36. Nunthaboot, N.; Rungrotmongkol, T.; Malaisree, M.; Decha, P.; Kaiyawet, N.; Intharathep, P.; Sompornpisut, P.; Poovorawan, Y.; Hannongbua, S., Molecular insights into human receptor binding to 2009 H1N1 influenza A hemagglutinin. *Monatsh. Chem.* **2009,** accepted.

37. http://www.ncbi.nlm.nih.gov/genomes/FLU/SwineFlu.html.

38. *Discovery Studio 2.0,* Accelrys Inc: San Diego, CA, USA.

39. Li, H.; Robertson, A. D.; Jensen, J. H., Very fast empirical prediction and rationalization of protein pKa values. *Proteins.* **2005,** 61, 704-721.

40. Bas, D. C.; Rogers, D. M.; Jensen, J. H., Very fast prediction and rationalization of pKa values for protein-ligand complexes. *Proteins.* **2008,** 73, 765-783.

41. Darden, T.; York, D.; Pedersen, L., Particle mesh Ewald: an N·log(N) method for Ewald sums in large systems. *J. Chem. Phys.* **1993,** 98, 10089-10092.

42. Ryckaert, J.-P.; Ciccotti, G.; Berendsen, H. J. C., Numerical integration of the cartesian equations of motion of a system with constraints: molecular dynamics of n-alkanes. *J. Comput. Phys.* **1977,** 23, 327-341.

43. Ha, Y.; Stevens, D. J.; Skehel, J. J.; Wiley, D. C., X-ray structures of H5 avian and H9 swine influenza virus hemagglutinins bound to avian and human receptor analogs. *Proc. Natl. Acad. Sci. USA.* **2001,** 98, 11181-11186.

44. Ha, Y.; Stevens, D. J.; Skehel, J. J.; Wiley, D. C., X-ray structure of the hemagglutinin of a potential H3 avian progenitor of the 1968 Hong Kong pandemic influenza virus. *Virology* **2003,** 309, 209-218.

45. Lin, T.; Wang, G.; Li, A.; Zhang, Q.; Wu, C.; Zhang, R.; Cai, Q.; Song, W.; Yuen, K.-Y., The hemagglutinin structure of an avian H1N1 influenza A virus. *Virology* **2009,** 392, 73-81.

46. Kumari, K.; Gulati, S.; Smith, D. F.; Gulati, U.; Cummings, R. D.; Air, G. M., Receptor binding specificity of recent human H3N2 influenza viruses. *Virology* **2007,** 4, 42-53.

47. Li, M. Y.; Wang, B. H., Computational studies of H5N1 hemagglutinin binding with SA-alpha-2, 3-Gal and SA-alpha-2, 6-Gal. *Biochem. Biophys. Res. Commun.* **2006,** 347, 662-668.

48. Xu, D.; Newhouse, E. I.; Amaro, R. E.; Pao, H. C.; Cheng, L. S.; Markwick, P. R. L.; McCammon, J. A.; Li, W. W.; Arzberger, P. W., Distinct Glycan Topology for Avian and Human Sialopentasaccharide Receptor Analogues upon Binding Different Hemagglutinins: A Molecular Dynamics Perspective. *J. Mol. Biol.* **2009,** 387, 465-491.

49. Iwata, T.; Fukuzawa, K.; Nakajima, K.; Aida-Hyugaji, S.; Mochizuki, Y.; Watanabe, H.; Tanaka, S., Theoretical analysis of binding specificity of influenza viral hemagglutinin to avian and human receptors based on the fragment molecular orbital method. *Comput. Biol. Chem.* **2008,** 32, 198-211.

50. Lin, T.; Wang, G.; Li, A.; Zhang, Q.; Wu, C.; Zhang, R.; Cai, Q.; Song, W.; Yuen, K. Y., The hemagglutinin structure of an avian H1N1 influenza A virus. *Virology* **2009,** 392, 73-81.

51. Kumari, K.; Gulati, S.; Smith, D. F.; Gulati, U.; Cummings, R. D.; Air, G. M., Receptor binding specificity of recent human H3N2 influenza viruses. *Virol J.* **2007,** 4, 42-53.

52. Li, M.; Wang, B., Computational studies of H5N1 hemagglutinin binding with SA-alpha-2, 3-Gal and SA-alpha-2, 6-Gal. *Biochem. Biophys. Res. Commun.* **2006,** 347, 662-668.

53. Xu, D.; Newhouse, E. I.; Amaro, R. E.; Pao, H. C.; Cheng, L. S.; Markwick, P. R.; McCammon, J. A.; Li, W. W.; Arzberger, P. W., Distinct Glycan Topology for Avian and Human Sialopentasaccharide Receptor Analogues upon Binding Different Hemagglutinins: A Molecular Dynamics Perspective. *J. Mol. Biol.* **2009,** 387, 465-491.

54. Soundararajan, V.; Tharakaraman, K.; Raman, R.; Raguram, S.; Shriver, Z.; Sasisekharan, V.; Sasisekharan, R., Extrapolating from sequence-the 2009 H1N1 'swine' influenza virus. *Nat. Biotechnol.* **2009,** 27, 510-513.

55. Coburn, B. J.; Wagner, B. G.; Blower, S., Modeling influenza epidemics and pandemics: insights into the future of swine flu (H1N1). *BMC. Med.* **2009,** 7, 30-37.

56. Munster, V. J.; Wit, E. d.; vandenBrand, J. M. A.; Herfst, S.; Schrauwen, E. J. A.; Bestebroer, T. M.; Vijver, D. v. d.; Boucher, C. A.; Koopmans, M.; Rimmelzwaan, G. F.; Kuiken, T.; Osterhaus, A. D.; Fouchier, R. A., Pathogenesis and Transmission of Swine-Origin 2009 A(H1N1) Influenza Virus in Ferrets. *Science.* **2009,** 325, 481-483.

57. Maines, T. R.; Jayaraman, A.; Belser, J. A.; Wadford, D. A.; Pappas, C.; Zeng, H.; Gustin, K. M.; Pearce, M. B.; Viswanathan, K.; Shriver, Z. H.; Raman, R.; Cox, N. J.; Sasisekharan, R.; Katz, J. M.; Tumpey, T. M., Transmission and Pathogenesis of Swine-Origin 2009 A(H1N1) Influenza Viruses in Ferrets and Mice. *Science* **2009,** 325, 484-487.

58. Chen, J.; Fang, F.; Yang, Z.; Liu, X.; Zhang, H.; Zhang, Z.; Zhang, X.; Chen, Z., Characterization of highly pathogenic H5N1 avian influenza viruses isolated from poultry markets in central China. *Virus. Res.* **2009,** 146, 19-28.

Appendices

สรุป Output จากโครงการวิจัยที่ได้รับทุนจาก สกว.

1. ผลงานตีพิมพ์ในวารสารวิชาการนานาชาติ 2 ฉบับ

- **Nadtanet Nunthaboot**, Thanyada Rungrotmongkol, Maturos Malaisree, Panita Decha Nopporn Kaiyawet, Pathumwadee Intharathep, Pornthep Sompornpisut, Yong Poovorawan, Supot Hannongbua. Molecular insights into human receptor binding to 2009 H1N1influenza A hemagglutinin. Monatsh Chem (2010) 141:801–807. (impact factor 1.31)
- **Nadtanet Nunthaboot**, Thanyada Rungrotmongkol, Maturos Malaisree, Nopporn Kaiyawet, Panita Decha, Pornthep Sompornpisut, Yong Poovorawan, and Supot Hannongbua Evolution of Human Receptor Binding Affinity of H1N1 Hemagglutinins from 1918 to 2009 Pandemic Influenza A Virus. *J. Chem. Inf. Model.* (2010) 50:1410-1417. (impact factor 3.88)

2. การนำผลงานวิจัยไปใช้ประโยชน์

ได้มีการนำข้อมูลที่ได้จากงานวิจัยดังกล่าวไปใช้ประโยชน์ในแง่

- เชิงสาธารณะ เนื่องจากการระบาดของเชื้อไข้หวัดใหญ่สายพันธ์ใหม่ 2009 H1N1 นั้นได้ก่อให้เกิดความหวาดกลัวและตื่นตระหนกเป็นอย่างมาก จากการศึกษาสมบัติทางโครงสร้างและทางพลวัติของไกลโคโปรตีนฮีมแมกกลูตินินของไข้หวัดใหญ่สายพันธ์ใหม่ 2009 H1N1 ในระดับเชิงอะตอม บทบาทสำคัญของกรดอะมิโนที่ตำแหน่งการยึดจับ รวมทั้งอันตร-กิริยาที่เกิดขึ้นระหว่างโปรตีนฮีมแมกกลูตินินกับตัวรับ ซึ่งการให้ความรู้พื้นฐานที่สำคัญเหล่านี้จะช่วยให้ประชาชนไม่ตื่นตระหนกเกี่ยวกับเชื้อไวรัสไข้หวัดใหญ่สายพันธุ์ใหม่ที่ระบาดอยู่ในปัจจุบัน รวมทั้งประชาชนยังมีความรู้ความเข้าใจมากยิ่งขึ้นเกี่ยวกับกระบวนการแพร่พันธ์ของเชื้อไวรัสไข้หวัดดังกล่าว ตลอดจนสามารถใช้เป็นข้อมูลในการติดตามการกลายพันธ์หรือการอุบัติขึ้นของไข้หวัดสายพันธ์ใหม่ในปีต่อๆ นอกจากนี้งานวิจัยนี้ยังเป็นการสร้างเครือข่ายความ

ร่วมมือกับอาจารย์จากคณะแพทยศาสตร์ จุฬาลงกรณ์มหาวิทยาลัย ซึ่งให้ข้อมูลทางด้านอณูชีววิทยาของเชื้อไวรัสไข้หวัด

- เชิงวิชาการ ได้มีการนำเนื้อหาบางส่วนของงานวิจัยมาประยุกต์ใช้ในการเรียนการสอน โดยเฉพาะวิชาทางเคมีคำนวณ เพื่อให้นักศึกษามีความรู้ความเข้าใจและสามารถประยุกต์ใช้หลักการหรือทฤษฎีทางเคมีได้

3. มีการนำงานวิจัยนี้ไปเสนอผลงานแบบบรรยาย ในงานประชุมวิชาการ ดังนี้

- Effects of Residues Changes on Human Receptor Binding Affinity of H1N1 Hemagglutinins: Insights from Molecular Dynamics Simulation ในงานประชุมวิชาการนานาชาติทางวิทยาการและวิศวกรรมทางคอมพิวเตอร์ประจำปี ครั้งที่ 14 (ANSCSE14) ระหว่างวันที่ 23-26 มีนาคม 2553 ณ มหาวิทยาลัยแม่ฟ้าหลวง จังหวัดเชียงราย
- Changes of human receptor binding affinity of H1N1 hemagglutinins: Insights from molecular dynamics simulation ในการประชุมวิชาการ 240th ACS National Meeting ในระหว่างวันที่ 22-26 สิงหาคม 2553 ณ เมืองบอสตัน ประเทศสหรัฐอเมริกา

Monatsh Chem (2010) 141:801–807
DOI 10.1007/s00706-010-0319-z

ORIGINAL PAPER

Molecular insights into human receptor binding to 2009 H1N1 influenza A hemagglutinin

Nadtanet Nunthaboot · Thanyada Rungrotmongkol · Maturos Malaisree · Panita Decha · Nopporn Kaiyawet · Pathumwadee Intharathep · Pornthep Sompornpisut · Yong Poovorawan · Supot Hannongbua

Received: 25 September 2009 / Accepted: 2 May 2010 / Published online: 27 May 2010

Abstract The current pandemic of the viral 2009 H1N1 influenza and its sustained human–human transmission has raised global concern for human health. The binding of the viral glycoprotein hemagglutinin (HA) and the human α-2,6-linked sialopentasaccharide (SIA-2,6-GAL) host cell receptor is a critical step in the viral replication cycle. Here, the complex structure of the 2009 H1N1 HA bound to the SIA-2,6-GAL sialopentasaccharide receptor was constructed by using homology modeling and molecular dynamic simulations. The receptor was found to fit very well within the HA binding pocket and formed hydrogen bonds with the residues of the 130-loop, 190-helix, and 220-loop. Most receptor binding residues play a significant role in stabilizing the protein–receptor complex with major contributions being provided by V135, T136, A137, K222, and Q226. The results are similar to the human SIA-2,6-GAL sialopentasaccharide receptor binding to H1 HA subtype, but are slightly different from those of H3, H5, and H9 HAs.

Keywords Computational chemistry · Hydrogen bonds · Molecular modelling · Sialopentasaccharide receptor · Per residue interactions · Molecular dynamics simulations

N. Nunthaboot
Department of Chemistry, Faculty of Science,
Mahasarakham University, Mahasarakham 44150, Thailand

T. Rungrotmongkol · M. Malaisree · P. Decha · N. Kaiyawet · P. Intharathep · P. Sompornpisut · S. Hannongbua (✉)
Computational Chemistry Unit Cell, Department of Chemistry,
Faculty of Science, Chulalongkorn University,
Bangkok 10330, Thailand
e-mail: supot.h@chula.ac.th

T. Rungrotmongkol
Center of Innovative Nanotechnology,
Chulalongkorn University, Bangkok 10330, Thailand

Y. Poovorawan
Center of Excellence in Clinical Virology,
Faculty of Medicine, Chulalongkorn University,
Bangkok 10330, Thailand

S. Hannongbua
Center of Excellence for Petroleum, Petrochemicals,
and Advanced Materials, Chulalongkorn University,
Bangkok 10330, Thailand

Introduction

Since the first identification of the novel A (H1N1) influenza virus in April 2009, the outbreak of this virus has rapidly spread and encircled over 100 countries worldwide, causing more than 3,000 human deaths (April–September 2009) [1]. The World Health Organization (WHO) announced a worldwide pandemic alert level at phase 6, indicating that a global human pandemic of this virus isolate is under way [1–3]. In the primary step of the viral replication cycle, influenza infection is initiated by the viral surface homotrimeric glycoprotein hemagglutinin (HA) binding to the host membrane sialylated glycans, which act as cell receptors. Understanding of this attachment and interaction can provide a basic knowledge of how the emerging virus infects humans and is thus the main goal of this study.

Hemagglutinin is an important target for the development of both vaccines and antiviral drugs against influenza viruses. Each monomer of the homotrimer is composed of two subunits, HA1 and HA2. Whilst HA1 is known to be responsible for the viral attachment to host cell, HA2 is associated with the release of the viral RNA complexed with the RNA polymerase through membrane fusion [4–7], and thus HA is essential to both host cell targeting and cell

entry (infection). HA1 binds to host cell membrane receptors, glycans containing the terminal sialic acid which are attached to surface membrane proteins or lipids [6, 8, 9]. The specific topology, determined principally but not exclusively by the specific linkage of the terminal sialic acid to the galactose subunit and the glycan chain length, identifies the species and tissue specificity and avidity of binding, and thus its infectability and transmission rates [10]. The avian influenza virus preferentially recognizes the sialic acid α-2,3-galactose (SIA-α-2,3-GAL) linkage with a long glycan chain and cone-like topology, whilst the adopted sialic acid α-2,6-galactose (SIA-α-2,6-GAL) linkage is more favorable for both human and swine influenza viruses with longer glycan chains and an umbrella topology [10–14]. It is supposed that the alternation in host specificity of sialic acid linked to galactose from α-2,3- to α-2,6-linkage is a major barrier for influenza viruses to cross species barriers and adapt to a new host [7, 10, 15–18].

From the available information, it is clear that the binding domain of HA with the glycan receptors comprises several key structural components including the 190-helix, 130- and 220-loop domains, and several other conserved residues that give species and tissue specificity [9]. However, how this is derived is not clear and to date, the H1N1-2009 HA structures, either as free-form or receptor-bound conformation, have not yet been experimentally solved. Recently, a theoretically modeled structure of the HA–receptor complex has been published [19]. However, it represents a static view of protein–receptor interactions without dynamic capture of time-dependent properties. Therefore, in the present study, molecular dynamics (MD) simulations were performed on the homology modeled structure of the novel H1N1 HA complexed with the SIA-2,6-GAL sialopentasaccharide, a human preferential receptor, to investigate the fundamental structural characteristics, the role of conserved binding residues, and receptor binding specificity. Extensive analysis was focused on the structural properties and, in particular, on the enzyme–receptor interactions in terms of hydrogen bonding and per residue–receptor interactions.

Results and discussion

MD simulation of the novel H1N1 HA complexed with the SIA-2,6-GAL sialopentasaccharide, a human preferential receptor, was carried out over a period of 4 ns. In the last 2.5-ns simulation, the whole system is fairly stable as indicated by the small magnitude of root mean square deviation (RMSD) fluctuation of ca. 0.5 Å (Fig. 1). The simulation run could thus provide a suitable basis for the subsequent analyses.

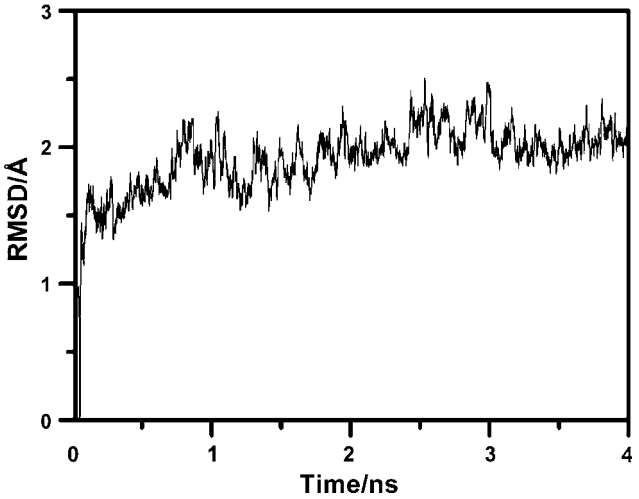

Fig. 1 Root mean square deviation (*RMSD*) of all heavy atoms of hemagglutinin and human SIA-α-2,6-GAL pentasaccharide receptor to the starting structure as a function of simulation time

The obtained human SIA-2,6-GAL sialopentasaccharide receptor was found to properly occupy the binding pocket of the 2009 H1N1 hemagglutinin, similar to what has been observed experimentally in the other viral influenza HA strains [21, 28–30], where the potentially important contact residues of the 130-loop (K133a, N133, V135, T136, and A137), 190-helix (H183, D190, and S193), and 220-loop (K222, D225, Q226, and E227) as well as Y95 (see Fig. 2a for residue positions) were revealed. Structural properties, hydrogen bonds, and per residue–receptor interactions are extensively discussed in the following sections.

Sialopentasaccharide receptor conformation

To investigate the conformational character of the human SIA-2,6-GAL sialopentasaccharide receptor, the distribution of eight important torsion angles, defined in Fig. 3a, from (1) *τ1–τ4* bridging between the saccharide units and (2) *τ5–τ8* of the functional groups of the terminal sialic acid, were measured and plotted in Fig. 3b and c, respectively.

It can clearly be seen in Fig. 3b that the *τ1* and *τ2* torsions of the first three saccharide units (SIA1, GAL2, and NAG3) show a single preferential and sharp peak, suggesting the high stability of these units which were well oriented and occupied in the binding pocket of the enzyme (Fig. 2a, b) and, therefore, that many hydrogen bonds with the HA residues were firmly formed (Fig. 4a, discussed later). The most probable glycosidic torsion angle (*τ1*, black line in Fig. 3b) was found at ca. −68° indicating the adopted *cis*-conformation of the α-2,6-linked terminal sialic acid (SIA1) to the galactose (GAL2) of the receptor. This proposed conformation is consistent with what has

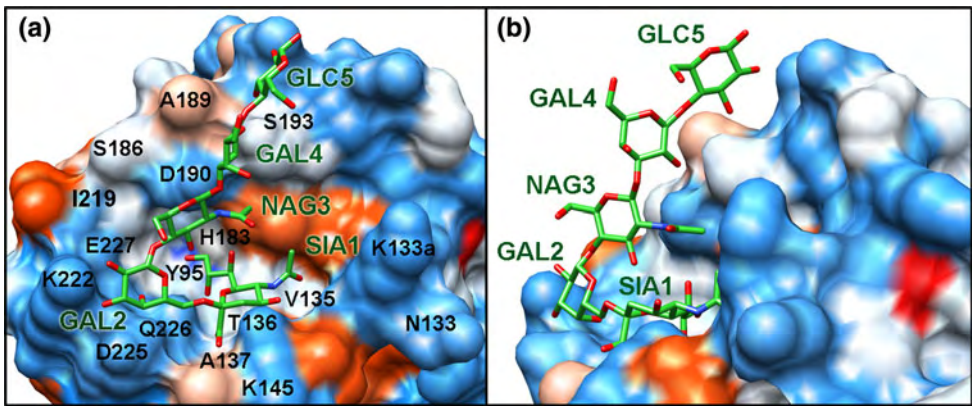

Fig. 2 **a** Top and **b** side views of the human SIA-2,6-GAL sialopentasaccharide receptor bound to the binding pocket of the 2009 H1N1 influenza HA. The potential contact residues and five units of the receptor (SIA1, GAL2, NAG3, GAL4, and GLC5) are labeled. Residue K133a is an inserted amino acid specific to the 2009 H1N1 HA. *Blue* and *orange* surfaces indicate the hydrophilic and hydrophobic features, respectively (color figure online)

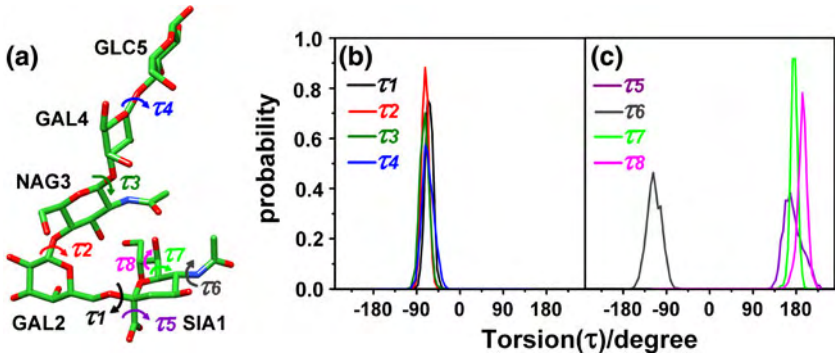

Fig. 3 **a** Definition of torsion angles of the human SIA-2, 6-GAL sialopentasaccharide receptor. Probability distributions of the **b** torsion angles ($\tau 1$–$\tau 4$) linking between each saccharide unit and **c** torsion angles ($\tau 5$–$\tau 8$) of the functional groups of the terminal sialic acid

been observed both experimentally and theoretically for the human SIA-2,6-GAL receptor binding to the influenza HA subtypes H1, H3, and H5, whose glycosidic torsion angles were observed to fall within the range of between −50° and −70° [21, 30–33]. In the same fashion, the $\tau 3$ and $\tau 4$ angles linking between the last three saccharides (NAG3, GAL4, and GLC5) showed the single preferential sharp peak at ca. −73° (Fig. 3b) indicating their high rigidity throughout the simulation period.

To reveal the conformational change of the terminal sialic acid SIA1, the torsion angles of its functional groups were further evaluated and the results are shown in Fig. 3c. Amongst the four angles, $\tau 5$ and $\tau 6$ are slightly broader than the other two angles, $\tau 7$ and $\tau 8$. This indicates that the –COO– and –NHAc groups could feasibly rotate rather than the hydrophilic group.

Enzyme–receptor hydrogen bonds

To determine the protein–receptor interactions, hydrogen bonding between the HA residues and the human SIA-α-2,6-GAL sialopentasaccharide receptor were calculated according to the two criteria: (1) a proton donor (D) and acceptor (A) distance of 3.5 Å or less and (2) a D–H···A angle of 120° or more.

The number and percentage of hydrogen bond occupation of each of the 2009 HA binding residues and all five saccharides of the receptor were evaluated, and the results are shown in Fig. 4a (see description in Table 1). At the terminal sialic acid (SIA1, see Fig. 2a), extensive interactions were found with Y95 and the highly conserved residues of the 130-loop (V135, T136, and A137), 190-helix (H183), and 220-loop (Q226). The hydroxyl oxygen of the hydrophilic group forms a strong hydrogen bond to the phenyl group of Y95. Three strong hydrogen bonds were detected between the terminal sialic acid –COO^- group and the three HA residues, T136 and A137 in the 130-loop and Q226 in the 220-loop, whilst the –NHAc moiety established two strong hydrogen bonds with the backbone nitrogen and oxygen atoms of residue V135 in the 130-loop. In addition, the hydroxyl oxygen atoms of hydrophilic side chain form strong and moderate hydrogen bonds with the imidazole ring of H183 in the 190-helix and the amide group of Q226 in the 220-loop, respectively.

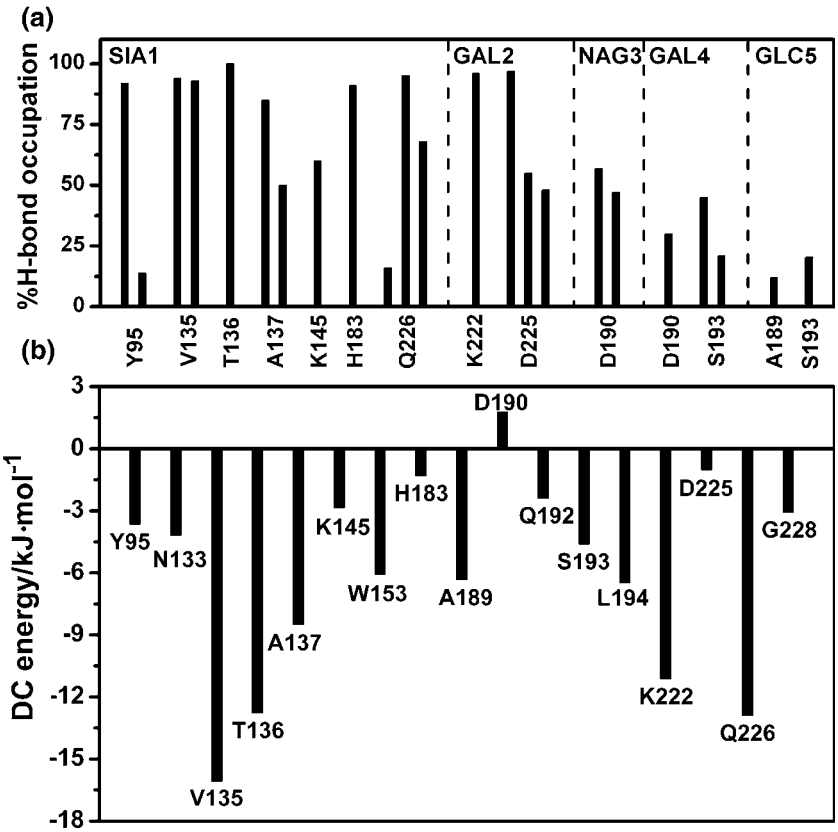

Fig. 4 **a** Hydrogen bonding occupation and **b** decomposition (*DC*) energy in kJ mol^{-1} of the individual residues of the 2009 H1N1 HA towards the human SIA-2,6-GAL sialopentasaccharide receptor (see Fig. 2 for residue labels)

Based on the numbers of hydrogen bonds (see Fig. 4a), the 130-loop is more likely to be in contact with SIA1 than the 190-helix and 220-loop, which is comparable to that of the other hemagglutins complexed with the human receptor [21, 30, 33].

For the second unit of the human SIA-2,6-GAL sialopentasaccharide receptor (GAL2), two strong hydrogen bonds were formed with the ammonium group of K222 and the backbone oxygen of D225. These hydrogen bonds were also detected in the case of the H5 HA–receptor complex, but not in the H3 and H9 HA–receptor complexes [33]. Moreover, two moderate hydrogen bonding interactions between the hydroxyl moieties of this saccharide and the carboxylate group of D225 were also found. Instead, G225, as in the crystal structure of the H1 HA–receptor complex [21, 30], forms hydrogen bonds through its backbone oxygen with the GAL2 unit. Finally, considering the other three units (NAG3, GAL4, and GLC5) of the sialopentasaccharide, they were all found to establish medium to rather weak hydrogen bond networks to the two 190-helix residues, D190 and S193, which are in agreement with the published results of the swine H1–receptor structure [21]. Interestingly, they are, however, different from what has been reported for the H3, H5, and H9 HA–receptor complexes where the last three glycans explicitly interact with the 150-loop and 190-helix [33].

Taking into account all the simulation results shown above, all important hydrogen bonds between the SIA-2,6-GAL sialopentasaccharide receptor and the residues of the 130-loop, 190-helix, and 220-loop are considerably conserved and are more likely to be similar to those observed in the H1 HA–receptor complex structure [21, 30], indicating the likely reliability of the simulated structures of the human receptor bound to the pocket of the viral H1N1-2009 HA. In addition, the results also confirm the potentially important role of the 130-loop, 190-helix, and 220-loop of the viral surface HA in attaching to SIA-2,6-GAL sialopentasaccharide glycan, which is the main receptor found in human respiratory tract host cells.

Per residue HA enzyme–SIA-2,6-GAL receptor interactions

To reveal the fundamental basis of the binding between the human SIA-2,6-GAL sialopentasaccharide receptor and the influenza HA, the interaction energies between each of the individual residues and the SIA-2,6-GAL sialopentasaccharide were evaluated by using the decomposition (DC) energy module implemented in AMBER 10. The energetic contribution was averaged over a set of 100 MD snapshots, taken at every 25 ps from the last 2.5-ns simulation.

Table 1 Hydrogen bond descriptions and interactions detected between heavy atoms of the human SIA-α-2,6-GAL pentasaccharide receptor and 2009-H1N1 hemagglutinin residues

Pentasaccharide	HA	Type	Occupation (%)
SIA1	Y95	Y95_OH_H···O8_SIA1	92
	Y95	Y95_OH···H_O9_SIA1	14
	V135	V135_N_H···O5N_SIA1	94
	V135	V135_O···H_N5_SIA1	93
	T136	T136_OG1_H···O1B_SIA1	100
	A137	A137_N_H···O1A_SIA1	85
	A137	A137_N_H···O1B_SIA1	50
	K145	K145_NZ_H···O4_SIA1	60
	H183	H183_NE2···H_O9_SIA1	91
	Q226	Q226_NE2_H···O1A_SIA1	16
	Q226	Q226_NE2_H···O1B_SIA1	95
	Q226	Q226_OE1···H_O8_SIA1	68
GAL2	K222	K222_NZ_H···O3_GAL2	96
	D225	D/G225_O···H_O4_GAL2	97
	D225	D225_OD1···H_O3_GAL2	55
	D225	D225_OD2···H_O3_GAL2	48
NAG3	D190	D190_OD1···H_N2_NAG2	57
	D190	D190_OD2···H_N2_NAG2	47
GAL4	D190	D190_OD1···H_O2_GAL4	30
	S193	S193_OG···H_O2_GAL4	45
	S193	S193_OG_H···O2_GAL4	21
GLC5	A189	T189_O···H_O6_GLC5	12
	S193	S193_OG···H_O3_GLC5	20

The evaluated DC energies of the HA residues located in the binding pocket are plotted in Fig. 4b, where the per residue interaction energies are seen to vary within the range of 2 to -17 kJ mol^{-1}. The major contribution to the enzyme–receptor interactions was gained from the conserved residues which are the members of the 130- and 220-loops: V135, T136, A137, K222, and Q226. The corresponding DC energies of less than -8 kJ mol^{-1} due to these residues agree well with the hydrogen bond data discussed above (Fig. 4a) and corroborate their important role in attaching the viral coat HA to the human SIA-2,6-GAL sialopentasaccharide receptor of susceptible host cells. The higher negative values of the DC data in Fig. 4b for the remaining residues of these two loops and the 190-helix residues (except for D190) also indicate their likely responsibilities in stabilizing the human receptor–HA complex. In some contrast, and in agreement with a previous theoretical report [34], the D190 residue was found to destabilize the protein–receptor complex.

Interestingly, as determined from their DC energies, the D225 and D190 residues do not significantly improve the enzyme–receptor binding affinity, although they interact explicitly via three hydrogen bonds with the GAL2, NAG3, and GAL4 saccharides of the SIA-2,6-GAL sialopentasaccharide, respectively (as discussed above). This can then be best understood in terms of their total interactions with the neighboring residues, since the DC energy is a summation of all interactions between a central residue and its environment, including the SIA-2,6-GAL receptor and all the residues of the respective HA enzyme. In other words, the D225 and D190 hydrogen bond energies can be destabilized by their repulsions with the other residues of the HA.

Conclusions

In the present study, the three-dimensional structure of the human SIA-2,6-GAL sialopentasaccharide receptor bound to the recently detected 2009 H1N1 HA was modeled based on a homology modeling approach and consequently performed by molecular dynamic simulations. The structural properties and protein–receptor interactions, in terms of the receptor conformation, hydrogen bonds, and per residue interaction energies, were extensively discussed and compared to the binding between the human SIA-2,6-GAL sialopentasaccharide receptor and the other HAs. Basically, comparative molecular dynamics are complementary to experimental results (tissue binding, glycan microarrays, Scatchard analysis) and do not suffer the drawback of crystallographic methods in that the glycan and HA protein show considerable flexibility in conformation which is missed, by being only a single snapshot, by crystallography methods.

Conformational analysis of the human SIA-2,6-GAL sialopentasaccharide receptor orientation throughout the simulation period confirms the adopted preferential *cis*-conformation of this receptor, as indicated by the glycosidic torsion angle between the terminal sialic acid (SIA1) and the adjacent galactose (GAL2) of ca. $-68°$. The simulated model of the 2009 H1 HA bound to the human SIA-2,6-GAL sialopentasaccharide receptor showed a well-oriented conformation of the receptor in the binding pocket of the HA enzyme and lays in the conserved regions including the 130-loop, 190-helix, and 220-loop. The sialic acid forms many strong hydrogen bonds with the HA residues V135, T136, A137, H183, and Q226. Furthermore, the GAL2 unit of the receptor was found to interact with the HA K222 and D225 residues, whilst the last three glycans established hydrogen bonds with D190 and S193. Based on a per residue interaction analysis, most receptor binding residues (especially V135, T136, A137, K222, and Q226) of the viral surface HA were found to play a stabilizing role in attaching to the human SIA-2,6-GAL sialopentasaccharide receptor of the host cell.

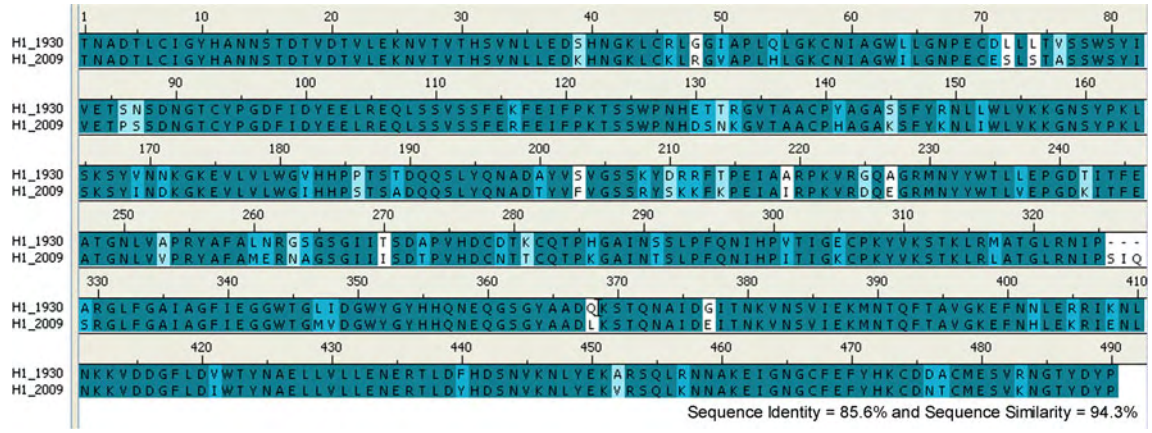

Fig. 5 Sequence alignment of 1930 and 2009 H1 hemagglutinins of influenza A (H1N1) viruses

In comparison to the other influenza HAs–human SIA-2,6-GAL sialopentasaccharide receptor complexes, the simulated results of this receptor binding to the 2009 H1N1 influenza HA provided the highest similarity to those from the structure of the H1–receptor complex. This is mainly due to the fact that they belong to the identical HA subtype and so are likely to share the highest conformational as well as primary sequence similarity. In addition, the results also show somewhat similar properties to those evaluated and observed for the H3 and H5, and H9 HAs–SIA-2,6-GAL complexes. Although many experimental aspects of the 2009 H1N1 outbreak including its virulence and pandemic potential are still uncertain, our molecular information could provide a better understanding of the first step of the viral life cycle based on how the viral surface glycoprotein HA of the 2009 influenza A (H1N1) efficiently attaches and tightly binds with the human SIA-2,6-GAL sialopentasaccharide receptor.

Materials and methods

Model of 2009 H1N1 influenza hemagglutinin complexed with human receptor

The initial structure of the 2009 H1N1 influenza HA bound with the human SIA-2,6-GAL sialopentasaccharide receptor was modeled based on the sequence which was recently isolated from children in Southern California, A/California/04/2009(H1N1) [20]. To seek the most relevant structure of the 2009 HA protein, its amino acid sequence was preliminarily aligned to all seven available crystallographic H1N1 HA structures [21]. It was found that the highest amino acid sequence similarity, at 86% identical, was with the 1930 swine H1N1 HA structure (Fig. 5). Therefore, this HA enzyme structure complexed with the human SIA-2,6-GAL sialopentasaccharide receptor (Protein Data Bank entry code 1RVT) was chosen as the template [21] for building up the HA-2009 structure by homology modeling performed by using the module implemented in Discovery Studio 2.0 [22]. The novel H1N1 HA–receptor complex was then further refined by using energy minimization and followed by multiple stepwise MD simulations.

Molecular dynamics simulations

All simulations of HA–receptor complex were carried out using the SANDER module of the AMBER 10 software package [23]. The HA protein and SIA-2,6-GAL sialopentasaccharide were parameterized by using the AMBER03 [24] and the GLYCAM06 force fields [25], respectively. All missing hydrogen atoms were added by using the LEaP module [23] and the system was subsequently solvated by a cubic box with dimensions of $66 \times 69 \times 141$ Å^3 filled with TIP3P water molecules. Normal charge states of ionizable amino acids corresponding to pH 7.0 were treated and 5 Cl^- counterions were further added to maintain neutrality on the system. A periodic boundary condition in the isobaric–isothermal (NPT) ensemble with a constant pressure of 1 atm and a temperature of 310 K was set up, whilst a Berendsen coupling time of 0.2 ps was employed to control the temperature. The SHAKE algorithm [26] was applied to constrain all hydrogen bonds using a time step of 2 fs. Non-bonded interactions were calculated with a 12-Å residue-based cutoff and the particle mesh Ewald method [27] was applied to treat the long-range electrostatic interactions. To remove unfavorable contact, the structure of the HA–receptor complexes was relaxed by performing 3,000 steps of conjugated gradient energy minimization. The whole system was subsequently heated from 0 to 310 K over 100 ps. The system was pre-equilibrated for two steps of 200-ps simulations with position restraints on the receptor atoms with the factors of 80 and 40 kJ mol^{-1} Å^{-2},

to maintain their coordinates inside the protein binding pocket. Afterwards, the complex was fully simulated for 4 ns.

Acknowledgments This work was financially supported by the Thailand Research Fund (TRF) and the Commission Higher Education (CHE). N.N. (Grant No. MRG5180298) and T.R. (Grant No. TRG5280035) acknowledge the funding for New Research from TRF. The authors are grateful for the partial support by the Rachadapisek Sompoch Endowment Fund "Emerging Health Risk Cluster", Chulalongkorn University. The Center of Excellence for Petroleum, Petrochemicals, and Advanced Materials, Chulalongkorn University, is acknowledged.

References

1. World Health Organization (2010) Global Alert and Response (GAR). http://www.who.int/csr/disease/swineflu/en/index.html. Accessed 2 May 2010
2. Zarocostas J (2009) World Health Organization declares A (H1N1) influenza pandemic. Available via http://www.bmj.com/cgi/content/extract/338/jun12_1/b2425. Accessed 2 May 2010
3. Centers for Disease Control and Prevention (2010) 2009 H1N1 flu. http://www.cdc.gov/h1n1flu/. Accessed 2 May 2010
4. Steinhauer DA (1999) Virology 258:1
5. Horimoto T, Kawaoka Y (2001) Clin Microbiol Rev 14:129
6. Cross KJ, Burleigh LM, Steinhauer DA (2001) Exp Rev Mol Med 6:1
7. Stevens J, Blixt O, Tumpey TM, Taubenberger JK, Paulson JC, Wilson IA (2006) Science 312:404
8. Wiley DC, Skehel JJ (1987) Annu Rev Biochem 56:365
9. Skehel JJ, Wiley DC (2000) Anun Rev Biochem 69:531
10. Chandrasekaran A, Srinivasan A, Raman R, Viswanathan K, Raguram S, Tumpey TM, Sasisekharan V, Sasisekharan R (2008) Nat Biotechnol 26:107
11. Bateman AC, Busch MG, Karasin AI, Bovin N, Olsen CW (2008) J Virol 82:8204
12. Gambaryan AS, Karasin AI, Tuzikov AB, Chinarev AA, Pazynina GV, Bovin NV, Matrosovich MN, Olsen CW, Klimov AI (2005) Virus Res 114:15
13. Matrosovich MN, Gambaryan AS, Teneberg S, Piskarev VE, Yamnikova SS, Lvov DK, Robertson JS, Karlsson KA (1997) Virology 233:224
14. Rogers GN, D'Souza BL (1989) Virology 173:317
15. Suzuki Y, Ito T, Suzuki T, Holl RE, Chambers TM, Kiso M, Ishida H, Kawaoka Y (2000) J Virol 74:11825
16. Russell RJ, Stevens DJ, Haire LF, Gamblin SJ, Skehel JJ (2006) Glycoconjugate J 23:85
17. van Riel D, Munster VJ, de Wit E, Rimmelzwaan GF, Fouchier RA, Osterhaus AD, Kuiken T (2007) Am J Pathol 171:1215
18. Nicholls JM, Bourne AJ, Chen H, Guan Y, Peiris JSM (2007) Respir Res 8:73
19. Soundararajan V, Tharakaraman K, Raman R, Raguram S, Shriver Z, Sasisekharan V, Sasisekharan R (2009) Nat Biotechnol 27:510
20. National Center for Biotechnology Information (NCBI) (2010) GenBank sequences from pandemic (H1N1) 2009 viruses. http://www.ncbi.nlm.nih.gov/genomes/FLU/SwineFlu.html. Accessed 2 May 2010
21. Gamblin SJ, Haire LF, Russell RJ, Stevens DJ, Xiao B, Ha Y, Vasisht N, Steinhauer DA, Daniels RS, Elliot A, Wiley DC, Skehel JJ (2004) Science 303:1838
22. Discovery Studio 2.0, Accelrys Inc., San Diego, CA, USA
23. Case DA, Darden TA, Cheatham TE, Simmerling CL, Wang J, Duke RE, Luo R, Crowley M, Walker RC, Zhang W, Merz KM, Wang B, Hayik S, Roitberg A, Seabra G, Kolossváry I, Wong KF, Paesani F, Vanicek J, Wu X, Brozell SR, Steinbrecher T, Gohlke H, Yang L, Tan C, Mongan J, Hornak V, Cui G, Mathews DH, Seetin MG, Sagui C, Babin V, Kollman PA (2008) AMBER 10, University of California, San Francisco
24. Duan Y, Wu C, Chowdhury S, Lee MC, Xiong G, Zhang W, Yang R, Cieplak P, Luo R, Lee T, Caldwell J, Wang J, Kollman P (2003) J Comput Chem 24:1999
25. Tessier MB, DeMarco ML, Yongye AB, Woods RJ (2008) Mol Simulat 34:349
26. Ryckaert JP, Ciccotti G, Berendsen HJC (1977) J Comput Phys 23:327
27. Darden T, York D, Pedersen L (1993) J Chem Phys 98:10089
28. Ha Y, Stevens DJ, Skehel JJ, Wiley DC (2001) Proc Natl Acad Sci U S A 98:11181
29. Ha Y, Stevens DJ, Skehel JJ, Wiley DC (1968) Virology 309:209
30. Lin T, Wang G, Li A, Zhang Q, Wu C, Zhang R, Cai Q, Song W, Yuen KY (2009) Virology 392:73
31. Kumari K, Gulati S, Smith DF, Gulati U, Cummings RD, Air GM (2007) Virol J 4:42
32. Li MY, Wang BH (2006) Biochem Biophys Res Commun 347:662
33. Xu D, Newhouse EI, Amaro RE, Pao HC, Cheng LS, Markwick PRL, McCammon JA, Li WW, Arzberger PW (2009) J Mol Biol 387:465
34. Iwata T, Fukuzawa K, Nakajima K, Aida-Hyugaji S, Mochizuki Y, Watanabe H, Tanaka S (2008) Comput Biol Chem 32:198

Evolution of Human Receptor Binding Affinity of H1N1 Hemagglutinins from 1918 to 2009 Pandemic Influenza A Virus

Nadtanet Nunthaboot,[†] Thanyada Rungrotmongkol,[‡,§] Maturos Malaisree,[‡] Nopporn Kaiyawet,[‡] Panita Decha,[||] Pornthep Sompornpisut,[‡] Yong Poovorawan,[⊥] and Supot Hannongbua*[,‡]

Department of Chemistry, Faculty of Science, Mahasarakham University, Mahasarakham, 44150, Thailand, Computational Chemistry Unit Cell, Department of Chemistry, Faculty of Science, Chulalongkorn University, Bangkok, 10330, Thailand, Center of Innovative Nanotechnology, Chulalongkorn University, Bangkok, 10330, Thailand, Computational Chemistry Research Unit, Department of Chemistry, Faculty of Science, Thaksin University, Phatthalung 93110, Thailand, and Center of Excellence in Clinical Virology, Faculty of Medicine, Chulalongkorn University, Bangkok, 10330, Thailand

Received January 27, 2010

The recent outbreak of the novel 2009 H1N1 influenza in humans has focused global attention on this virus, which could potentially have introduced a more dangerous pandemic of influenza flu. In the initial step of the viral attachment, hemagglutinin (HA), a viral glycoprotein surface, is responsible for the binding to the human SIA α2,6-linked sialopentasaccharide host cell receptor (hHAR). Dynamical and structural properties, based on molecular dynamics simulations of the four different HAs of Spanish 1918 (H1-1918), swine 1930 (H1-1930), seasonal 2005 (H1-2005), and a novel 2009 (H1-2009) H1N1 bound to the hHAR were compared. In all four HA−hHAR complexes, major interactions with the receptor binding were gained from HA residue Y95 and the conserved HA residues of the 130-loop, 190-helix, and 220-loop. However, introduction of the charged HA residues K145 and E227 in the 2009 HA binding pocket was found to increase the HA−hHAR binding efficiency in comparison to the three previously recognized H1N1 strains. Changing of the noncharged HA G225 residue to a negatively charged D225 provides a larger number of hydrogen-bonding interactions. The increase in hydrophilicity of the receptor binding region is apparently an evolution of the current pandemic flu from the 1918 Spanish, 1930 swine, and 2005 seasonal strains. Detailed analysis could help the understanding of how different HAs effectively attach and bind with the hHAR.

INTRODUCTION

The emerging influenza pandemic of the 2009 influenza A/H1N1 virus, with readily detected human−human transmission rates, has raised serious global concern for human health in recent times. Among the known targets determining the virus life's cycle, the initial step of viral attachment is mediated by HA binding the virion to the host cell receptor, α2,6 linked sialopentasaccharide (SIA-2,6-GAL; hHAR) in the case of humans. Amino acid mutations in the HA receptor binding domain could potentially introduce an outbreak of a new influenza virus. Relative to the 1918 Spanish (H1-1918), the 1930 swine (H1-1930), and the 2005 seasonal (H1-2005) H1N1 viruses, the HA binding pocket of the 2009 H1N1 (H1-2009) virus was found to display a notably higher hydrophilicity than the other three viral HAs. Such types of electronic effects, in cooperation with the structural differences due to the amino acid components (Table 1) in the binding pocket of the four HAs, are supposed to affect their susceptibility. A detailed and comparative understanding of the HA-hHAR binding among the four H1N1 strains is, then, the rational goal of this study.

On June 11, 2009, the WHO raised the alert status of the 2009 influenza A/H1N1 to level 6.[1] This novel H1N1 pandemic has caused at least 18 000 deaths in many countries around the world (as of July 2010). The most devastating influenza pandemic, 1918 H1N1 Spanish Flu, killed more than 40 million people worldwide.[2−4] The replication cycle of influenza virus is initiated by the attachment of the viral HA to sialylated glycans on the target cell-surface receptor, allowing for viral penetration into the host cell. While the adopted sialic acid α2,3-galactose linkage with a short glycan chain and cone-like topology is more favorable in avian influenza virus, the human and swine influenza viruses preferentially recognizes the sialic acid α2,6-galactose with longer glycan chains and an umbrella like topology,[5−10] hereafter referred to the hHAR. Besides HA functions, the M2-proton channel and neuraminidase (NA) are associated with the proton transport and the release of the newly synthesized viral particles in the viral replication cycle. Although the antiviral drugs approved against M2 ion channel and NA proteins are currently used for the treatment of influenza virus infections, the limitation of drug resistances because of amino acid mutations has led to an effort to

* To whom correspondence should be addressed. Tel: +66 22 187602. Fax: +66 22 187603. E-mail: supot.h@chula.ac.th.
[†] Department of Chemistry, Faculty of Science, Mahasarakham University.
[‡] Computational Chemistry Unit Cell, Department of Chemistry, Faculty of Science, Chulalongkorn University.
[§] Center of Innovative Nanotechnology, Chulalongkorn University.
[||] Computational Chemistry Research Unit, Department of Chemistry, Faculty of Science, Thaksin University.
[⊥] Center of Excellence in Clinical Virology, Faculty of Medicine, Chulalongkorn University.

10.1021/ci100038g
Published on Web 07/26/2010

Table 1. Comparison of Amino Acids in the HA Receptor Binding Domain of the Four Different H1N1 Influenza Viruses: The 1918 Spanish Flu (H1-1918), 1930 Swine Flu (H1-1930), 2005 Seasonal Flu (H1-2005), and 2009 Novel Flu (H1-2009)[a]

	H1N1 HA strains			
residue ID	H1-1918	H1-1930	H1-2005	H1-2009
95	Y	Y	Y	Y
133	T	T	**N**	**N**
133a	K	**R**	**R**	K
134	G	G	G	G
135	V	V	V	V
136	T	T	T	T
137	A	A	A	A
138	A	A	A	A
145	S	S	**N**	**K**
153	W	W	W	W
155	T	**V**	**V**	**V**
183	H	H	H	H
185	P	P	P	P
186	P	P	P	**S**
189	T	T	T	**A**
190	D	D	D	D
192	Q	Q	Q	Q
193	S	S	S	S
194	L	L	L	L
219	A	A	**E**	**I**
222	K	K	K	K
225	D	**G**	**G**	D
226	Q	Q	Q	Q
227	A	A	A	**E**
228	G	G	G	G

[a] Residues are numbered (residue ID) according to 1918 Spanish flu sequence. Using H1-1918 as the reference, the residue differences in the other three isolates are shown in bold and underlined. Residue K133a is an inserted amino acid specific to H1.

discover new potent inhibitors. Impacts of drug-resistant mutant strains of these two targeted proteins and their relevant commercial agents have been extensively studied.[11−14]

The viral genetic sequences in the HA receptor binding domain of the four different H1N1 influenza viruses, that is, the 1918 Spanish flu, 1930 swine flu, 2005 seasonal flu, and 2009 novel flu, are compared and are summarized in Table 1 (see multiple sequence alignment in Figure S1, Supporting Information). Using the original 1918 H1N1 HA as the reference, the amino acids at 7 Å spherical radius around the hHAR in the binding pockets of the H1-1930, H1-2005, and H1-2009 HAs contain three (K133aR, T155V, and D225G), six (T133N, K133aR, S145N, T155V, A219E, and D225G), and seven (T133N, S145K, T155V, P186S, T189A, A219I, and A227E) substitutions (shown in bold and underlined in Table 1), respectively. From a comparison of the hydrophobic plots (Figure 1), the 2009 HA binding pocket displays considerably higher hydrophilic characteristics (represented by the blue surface) than those of the other three HA strains. Since the residues 190 and 225 are known to be a key factor determining the HA−hHAR binding in all H1N1 subtypes,[15−20] and the HAs of all H1N1 strains contain D190, therefore, interest is focused on residue 225 in which G225 was found in the 1930 swine and 2005 seasonal viruses, whereas D225 was detected in the HAs of the two pandemic strains, H1-1918 and H1-2009 (Table 1). In addition, residue A227, which is the receptor binding site that is commonly conserved as "Q226-A227-G228" (QAG) was replaced by E227 in the novel 2009 influenza virus. Substitution of A227 by the negatively charged E227 residue (QEG) is supposed to affect the orientation of the surrounding residues.[18] As a consequence, the increase of the hydrophilicity and the replacement of the QAG by the QEG receptor binding site of the H1-2009 HA are possibly involved in the recognition and familiarity-strength in the binding to the hHAR of the newly emerged flu.

To examine the influence of the electronic and structural changes in the four HA binding pockets, molecular dynamics (MD) simulations of the hHAR bound to the four HA A/H1N1 influenza viruses were carried out. The HA−hHAR binding, as well as the structural and dynamical properties, were analyzed and are extensively discussed. The observed information at the atomic level could essentially provide a better understanding and a prediction of the new H1N1 influenza pathogenesis.

MATERIALS AND METHODS

System Preparation. The cocrystal structure of the 1930 swine influenza A/H1N1 HA (H1-1930) with the hHAR and the crystal structure of the apo form of the 1918 influenza A/H1N1 HA (H1-1918), were retrieved from the Protein Data Bank (PDB entry codes 1RVT and 1RUZ, respectively)[21] and were used as the starting structures for the MD simulations. To prepare the hHAR bound to the H1-1918 HA, superposition of the H1-1930 and the H1-1918 HA proteins over the backbone carbon atoms was performed, and the H1-1930 coordinates were then removed, retaining the coordinates of hHAR. The structure of the 2005 seasonal H1N1 HA complexed with the hHAR was prepared in a similar fashion of the H1-2009.[22] Briefly, using the structure of 1930 swine flu[21] as a template and amino acid sequences of the isolated Influenza A/swine/Chachoengsao/NIAH587/2005(H1N1),[23] the 3D-structure of the 2005 HA protein was created by homology modeling technique using the module implemented in Discovery Studio 2.0.[24] The hHAR bound to the H1-2005 HA was set up in a similar manner to that of the aforementioned H1-1918.

Molecular Dynamics Simulations. All calculations of the HA-hHAR complexes were carried out using the AMBER 10 software package.[25] The HA proteins and the hHAR were parametrized using the AMBER03[26] and GLYCAM06 force fields,[27] respectively. Protonation of the ionizable amino acids was assigned at pH 7.0 using the PROPKA program.[28,29] All missing hydrogen atoms were added using the LEaP module implemented in AMBER 10.[25] The simulated system was subsequently solvated by TIP3P water molecules in a cubic box with dimensions of $65 \times 68 \times 143$ Å^3 for H1-1918, $65 \times 68 \times 141$ Å^3 for H1-1930, and $67 \times 68 \times 141$ Å^3 for H1-2005. This is almost comparable to that of $66 \times 69 \times 141$ Å^3 used before for the H1-2009 complex.[22] The electroneutrality of the simulated systems was treated by adding 1, 0, 4, and 5 chloride counterions for H1-1918, H1-1930, H1-2005, and H1-2009, respectively. The periodic boundary condition in the isobaric−isothermal (NPT) ensemble with a constant pressure of 1 atm and temperature of 310 K was set up, whereas a Berendsen coupling time of 0.2-ps was employed to control the temperature. Nonbonded interactions were calculated with a 12 Å residue-based cutoff, and the Particle Mesh Ewald method[30] was applied to treat the long-range electrostatic interactions. A 2-fs step size with the SHAKE algorithm[31] was used along the simulations.

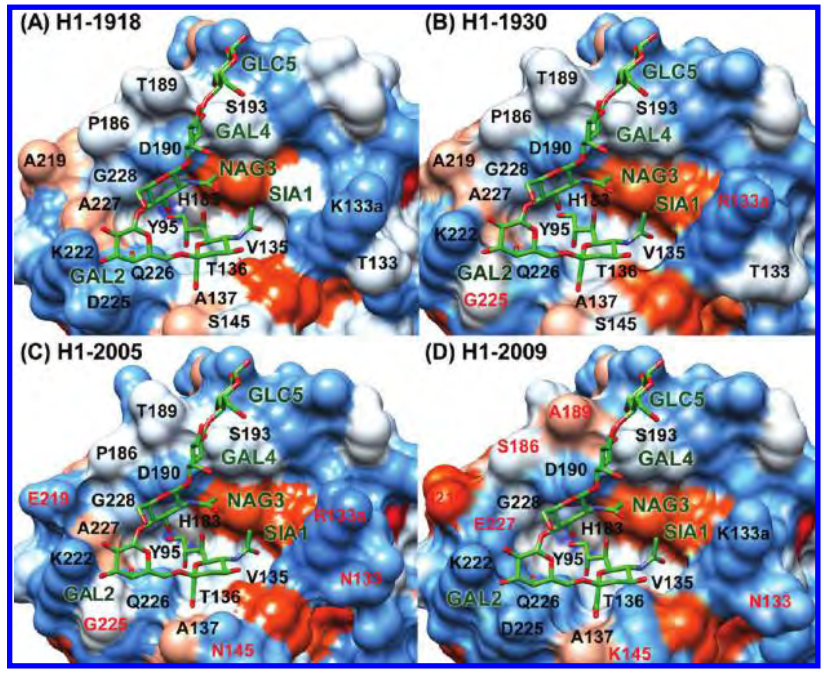

Figure 1. The hHAR in the binding pocket of the four viral influenza A/H1N1 HAs: (A) 1918 Spanish flu (H1-1918), (B) 1930 swine flu (H1-1930), (B) 2005 seasonal flu (H1-2005), and (D) 2009 novel pandemic flu (H1-2009). For H1-1930, H1-2005, and H1-2009, the residues that differ from the reference H1-1918 sequence are shown in red. The hydrophilic and hydrophobic surfaces are colored by blue and orange, respectively.

The water molecules were first relaxed with 500 steps of steepest descent (SD) and 1000 steps of conjugated gradient minimizations, while the HA and hHAR coordinates were kept fixed. The whole system was consequently optimized by performing 1,000 steps of SD and 1,000 steps of conjugated gradient minimizations. Afterward, the systems was heated to 310 K over 100-ps simulation and pre-equilibrated for 400 ps with position restraints on the hHAR atoms with factors of 20 and 10 kcal·mol^{-1}·Å^{-2} to maintain their coordinates inside the receptor-binding pocket. Finally, 6.5-ns simulations were carried out for each HA-hHAR complex and the structural coordinates from the last 5-ns (1.5−6.5-ns) simulations, a production period, were collected for analysis.

RESULTS AND DISCUSSION

Changes of the Receptor Conformation Inside the H1 Binding Pocket. The attachment of the viral surface homotrimeric glycoprotein HA to the host membrane via the hHAR is believed to be the primary step in the viral replication cycle. To differentiate the receptor's conformation in the binding pocket of the HAs of the Spanish flu (H1-1918), swine flu (H1-1930), seasonal flu (H1-2005), and a novel pandemic flu (H1-2009), the distributions of the torsion angles ($\tau1-\tau9$ in Figure 2) were measured and are plotted in Figure 3. As defined in Figure 2, $\tau1-\tau9$ were classified in three important regions providing three different characters of the receptor binding: (i) $\tau1-\tau3$, conformations of terminal sialic acid (SIA1) α2,6-linked to galactose (GAL2) of the hHAR; (ii) $\tau4-\tau6$, orientations of the three side chains of the SIA1 functional groups; and (iii) $\tau7-\tau9$, bridging between the saccharide units 2−5 of the receptor.

The distributions of the torsion angle plots (Figure 3), excluding $\tau9$ of H1-1930 and $\tau4$ of H1-2005, reveal clearly that all torsion angles of the four HA-hHAR systems show a sharp peak at almost the same position, suggesting that the hHAR adapts itself very well to reach its optimal structure within the four H1NI HA binding sites.

The $\tau1-\tau3$ angles on the single bonds linking between the six-membered rings of the SIA1 terminus and the GAL2 unit show a sharp peak at approximately −65°, −165° and 70°, respectively, indicating an identical orientation of these two sugars puckered into the HA pocket site. The $\tau1$ glycosidic torsion of approximately −65° represents their cis-conformation on the α-ketosidic linkage corresponding to those commonly observed in the SIA-α2,6-GAL receptor (hHAR) bound to other HAs by both experimental and theoretical studies.[21,32−35] Considering the orientations of the three side chains of the SIA1, the difference was only found at the carboxylate group of the H1-2005 in which its $\tau4$ was detected at ∼30° relative to ∼180° for the other HAs, that is, in difference from the other systems, the O1A group (see Figure 2) of the H1-2005 was rotated into the binding site to interact with the HA residues. The $\tau6$ angle of the hydrophilic moiety displayed a sharper peak than the $\tau4$ of the $-COO^-$ and $\tau5$ of the −NHAc groups, indicating that these two side chains are slightly more flexible in a narrow range in comparison with the hydrophilic group of the terminal SIA1.

For the remaining sugar moieties lying on the surface-exposed region of the hHAR protein (see Figure 1), the structural conformations of the NAG3 and GAL4 were found to be similar among the four HAs, as presented by the same degrees of $\tau7$ and $\tau8$ angles (−70° and −80°, respectively, in Figure 3). However, the orientation of the last glycan unit, GLC5, in the H1-1930 ($\tau9$ of 65°, red line) was somewhat different from the other three HAs ($\tau9$ of −65°). Therefore, different intermolecular interactions of the terminal GLC5 sugar of the saccharide chain with the protein surface residues

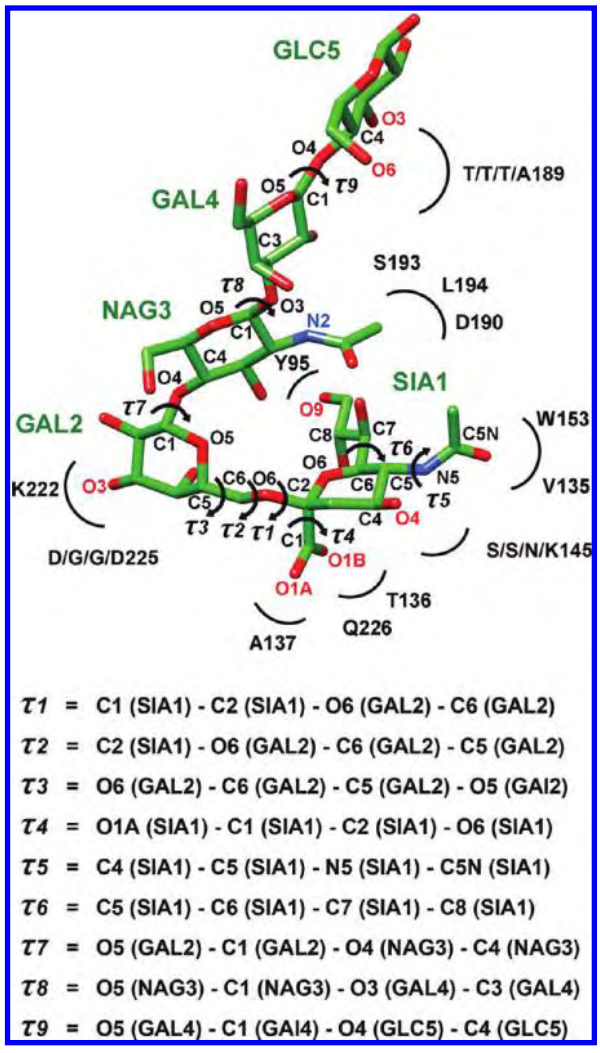

Figure 2. Schematic representation and definitions of the $\tau 1-\tau 9$ torsion angles of the hHAR in the binding site of the HA subtype H1. Some labeled atoms used in the results and discussion are also shown. The labels, such as S/S/N/K145, were used to represent the four different amino acids in the same sequence number of the 1918-, 1930-, 2005- and 2009-H1N1 HAs, respectively.

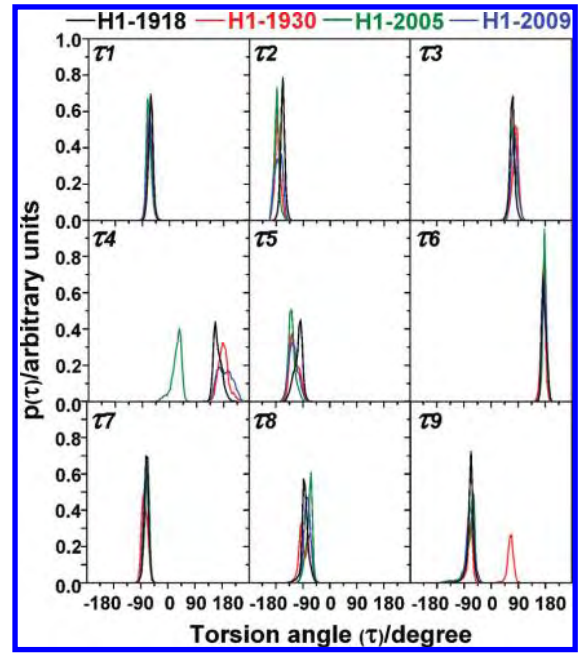

Figure 3. Distribution plots of the torsion angles ($\tau 1-\tau 9$) of the hHAR lying within the binding pocket of the HA of the four H1N1 strains (H1-1918, H1-1930, H1-2005, and H1-2009).

are to be expected in the H1-1930 case (details in the following sections).

Enzyme−Receptor Interactions. To gain insight into the efficiency of the hHAR binding to the HAs of H1-1918, H1-1930, H1-2005, and H1-2009, the percentage and number of hydrogen bonds between this receptor and the contact residues of HAs were measured according to the subsequent criteria: (i) the distance between proton donor (D) and acceptor (A) atoms of ≤ 3.5 Å and (ii) the D−H···A angle of $\geq 120°$. The results are shown in Figure 4 and the hydrogen bond descriptions are given in Table S1 (Supporting Information).

As shown in Figure 4, hydrogen bonds between the hHAR and the HA residues in all systems can be firmly formed in the three important binding HA regions, 130-loop, 190-helix, and 220-loop, especially at the sialic acid terminus which is inserted directly into the receptor-binding pocket of the HA. Strong hydrogen bonds are almost conserved at the residues Y95, V135, T136, A137, and Q226 of the four HA strains. Note that major interactions between the SIA1 and the T136 and Q226 are maintained although different hydrogen bonding pattern was detected, that is, the interaction takes place via the O1A in the H1-2005 and the O1B in the other HAs (see Table S1, Supporting Information). Noticeably change was found when the S/S/N145, a polar residue with noncharged side chain, in the H1-1918, H1-1930, and H1-2005 was replaced by the K145, a positively charged residue in a novel HA. This makes the H1-2009 capable of establishing one moderate hydrogen bond to the O4 of SIA1. The observed results lead to conclusion that introducing of the fourth lysine (K145) of the lysine fence (K133, K156, and K222) in the HA of the 2009 facilitates stronger enzyme−receptor binding by better anchoring the SIA1 terminus. This observation is in agreement with the recently proposed hypothesis.[36] Furthermore, a strong hydrogen bond between the H183 and the O9 of SIA1 was observed in the H1-1930, H1-2005, and H1-2009 complexes, whereas this kind of interaction was disappeared in the case of H1-1918 system.

A major difference was additionally found at the connecting GAL2 unit, where the number and percentage of hydrogen bonding interactions detected at the HA 220-loop on residues K222 and D/G/G/D225 are much stronger for H1-1918 and H1-2009 than those of H1-1930 and H1-2005 (Figure 4). It is clear that for the D/G/G/D225 binding, the direct electrostatic effects because of the negatively charged D225 residue, lead to a more effective interaction in the H1-1918 and the H1-2009 viral HAs than the noncharged G225 in the HA of the H1-1930 and H1-2005 viruses. For the K222-GAL2 binding, the moderate and strong hydrogen bonds between O3 of this particular unit and the K222 residue in the HA of H1-1918 and H1-2009 were observed. This is possibly affected by the indirect effects caused by the presence of one (D225) and two (D225 and E227) negatively charged residues (see also Table 1) in the binding pocket of H1-1918 and H1-2009, respectively. In 2009 influenza pandemic strain, the orientation of the K222 residue was mainly stabilized by both D225 and E227 residues through electrostatic and salt-bridge interactions, respectively

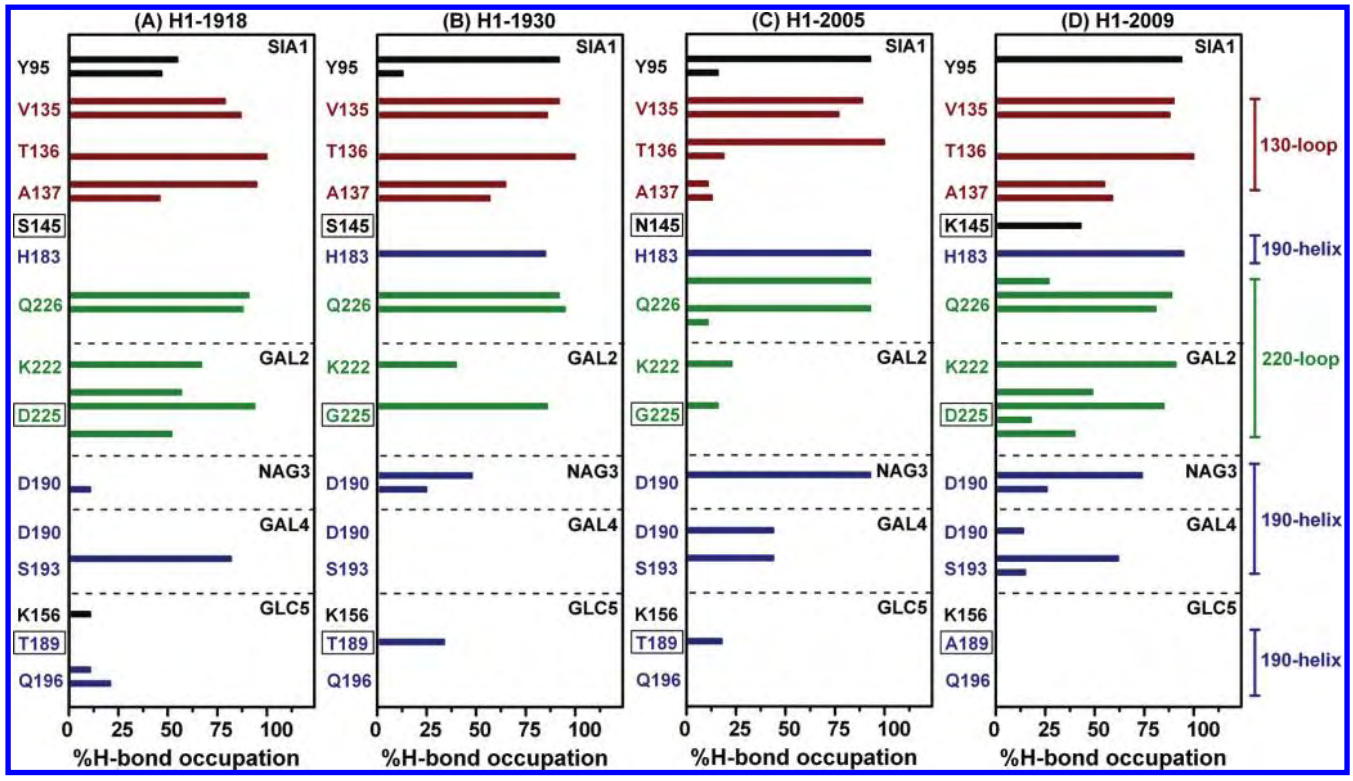

Figure 4. Hydrogen bond occupation between the five saccharide units (SIA1, GAL2, NAG3, GAL4, and GLC5) of the hHAR and the HA binding residues of (A) Spanish flu (H1-1918), (B) swine flu (H1-1930), (C) seasonal flu (H1-2005), and (D) a novel flu (H1-2009). The residues which are different among the four HAs are shown with a box around the label (see Figure 1 for residue positions). Residues of the 130-loop, 190-helix, and 220-loops are colored by red, blue, and green, respectively.

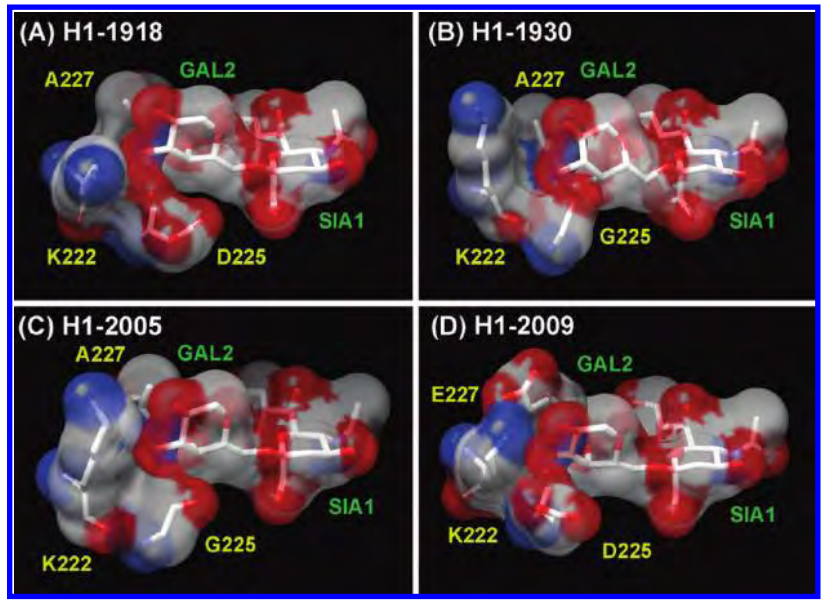

Figure 5. Electrostatic potential map of hHAR and HA binding residues K222, D/G/G/D225 and A/A/A/E227 of (A) Spanish flu (H1-1918), (B) swine flu (H1-1930), (C) seasonal flu (H1-2005), and (D) novel flu (H1-2009). Positive and negative electrostatic potentials are represented by blue and red, respectively.

(see Figure 5D and more discussion in the next section), whereas only D225 was observed to stabilize K222 in the case of H1-1918. This is in contrast with what was found for the H1-1930 and H1-2005 viruses, where both the G225 and A227 residues are hydrophobic, leading to a lowering of the electrostatic potential in this region, relative to those of the other two systems. This provides a clear reason why K222 could not form a stable hydrogen bond with GAL2 in the H1-1930 and H1-2005 HAs (Figure 4B and C, respectively). This hypothesis is further analyzed in terms of the electrostatic potential plot in the next section. A crucial role of residue 225 has been reported previously,[16−18] with the additional hypothesis that mutation of this residue could result in a reduced viral binding affinity to the hHAR. It has also been experimentally found that the presence of the G225 residue in the HA of H1-1930 and H1-2005 apparently reduced the binding efficiency of the virus to the hHAR.[3,16,18]

With respect to the NAG3, GAL4, and GLC5 saccharide units, which lay on the surface exposed region (Figure 1), far from the binding pocket, and are supposed to play only

a minor role in holding the receptor in place, a lower percentage and number of hydrogen bonds were found (Figure 4) in comparison to those observed at the first two units (SIA1 and GAL2) of the receptor. Their interactions were moderately strong with 190-helix residues T/T/T/A189, D190, and S193.

Taking into account all the above given data, the order of hydrogen bond strengths of the hHAR binding to the H1N1 HAs was H1-2009 > H1-1918 > H1-2005 ≅ H1-1930. The increase of binding affinity in the novel H1-2009 (H1N1) HA to the hHAR is mainly because of the higher hydrophilicity at the receptor binding domain, in which residues 145, 225, and 227 were found to play a critical role. The transmissibility of the 2009 H1N1 virus (depending upon several external factors and determined by the basic reproduction number, R_0 of 1.2−1.6) falls within the range of the 1918 Spanish flu (R_0 of 1.4−2.8) but is higher than that of seasonal influenza virus (R_0 of 0.9−2.1).[37,38] This transmission ability is supposed to relate, somewhat, to the predicted enzyme-receptor binding affinity. Note that the pathogenesis and transmission studies of the 2009 H1N1 influenza virus indicated that a novel flu was observed to be more pathogenic than the seasonal H1N1 virus.[38,39] Since the 2009 influenza virus could deeply penetrate into the airways and exhibits more extensive viral replication in the respiratory tract, its severity could potentially increase in comparison with seasonal virus.[38,39]

Effect of Charged Residues on the Receptor Binding Affinity. As already mentioned, hydrogen bond analysis revealed that introduction of charged amino acids in the receptor binding domain of the novel HA influenza virus could effectively contribute to the binding with the hHAR, in particular HA residues 222, 225, and 227. Therefore, to provide an additional perspective on the contribution of the polar residues to the hHAR-HA binding, the electrostatic isosurface maps of the hHAR and the HA 222, 225, and 227 residues were plotted in Figure 5. The positive and negative electrostatic potentials are indicated by blue and red, respectively.

In all systems, the negative electrostatic potentials (Figure 5, red) were found around the SIA1 and GAL2 units of the hHAR, while a positive electrostatic potential was generated over the K222 residue (Figure 5, blue). Differences between the four viral HAs are clearly and obviously observed in the region around the 225 and 227 residues. Here, changing the negatively charged D225 residue in the 1918- and 2009-H1N1 models to a nonpolar G225 residue (Table 1) leads to the negative electrostatic potential around residue 225 almost totally disappearing (the red regions in Figure 5A and D change to white in Figure 5B and C, respectively). In addition, the substitution of a nonpolar A227 residue of the 1918-, 1930-, and 2005-H1N1 HAs (Table 1) with a negatively charged E227 residue in the HA of H1-2009 leads additionally to an enhanced negative electrostatic potential around the 227 residue (the red region, which is only observed in Figure 5D).

As a consequence, the electrostatically negative potentials near residues D225 and E227 are unique in the H1-2009 H1N1 isolate (of the four studied) and the enhanced electronegative isosurface could potentially stabilize the ionic network of the 220-loop residues K222, D225, and E227. This helps the K222 residue to adjust its conformation to be in optimal contact with the GAL2 moiety of the hHAR, leading to the formation of a strong hydrogen bond in the H1-2009 HA−hHAR complex (Figure 4D), as previously discussed. On the other hand, the electrostatic potentials that result from the combination of the charged- and noncharged residues (D225 and A227) can potentially induce the moderate K222−GAL2 hydrogen bond formation in the H1-1918 HA−hHAR interaction (Figure 4A). This is not the case for the H1-1930 and H1-2005 HAs (Figure 4B and C, respectively), where this hydrogen bond is very weak because both G225 and A227 are fully uncharged and could not establish such ionic network with the K222.

Role of the Nonconserved Residue 227. Although residue 227 was found to vary between the influenza A viral strains, the receptor binding residues Q226 and G228 are highly conserved, forming a "Q226-X227-G228" pattern or so-called "QXG" site, where QSG and QGG sites are found in the avian H3 or H5 and H2 influenza virus HAs, respectively.[18,40] In this study, both the 1918-, 1930-, and 2005-H1N1 strains contain the QAG sequences, whereas the 2009-novel flu (H1-2009) shows a unique QEG site. The increased hydrophilicity in the receptor binding region is apparently the development of the current pandemic flu from the 1918 Spanish, the 1930 swine, and the seasonal 2005 influenzas. As shown and described in the previous sections, substitution of the noncharged A227 residue with the negatively charged E227 improves the binding of HA to the hHAR, and this is potentially attained by establishing the ionic network with the K222 and D225 residues. This finding thus indicates that the nonconserved residue 227 possibly plays a critical role in the evolution of a new and potentially more pathogenic H1N1 influenza virus. Note that among the three residues in the HA QXG site of the four H1 strains under this study, Q226 is the only residue that interacts directly with the hHAR via strong hydrogen bonds (Figure 4).

Human HAR Solvation. Solvation of the hHAR was monitored in terms of atom−atom radial distribution functions, RDFs, $g_{xy}(r)$, the probability of finding a particle of type y within a sphere radius r around the particle of type x. The RDFs from all heteroatoms of the hHAR to the oxygen atom of water were evaluated. The selected RDFs and the corresponding running coordination numbers, $n(r)$, are shown in Figure 6.

For all HA-hHAR complexes, the major differences in the $g(r)$ at the SIA1 terminus takes place only on the O1B atom (see Figure 2 for atomic label), where the plot for the H1-2005 complex shows the first sharp peak at ∼2.7 Å with the corresponding coordination number $n(r)$ integrated up to its first minimum of 2.8 water molecules (Figure 6B, right axis). This indicates that the water was firmly coordinated to the O1B atom of the H1-2005, but not in the HA-hHAR systems of H1-1918, H1-1930, and H1-2009. This is because of the interchange of the O1A and O1B positions due to the rotation of the $\tau 4$ angle (see Figure 3).

Although no significant difference was found in terms of the peak position of the RDFs of the other atoms of the SIA1 (Figure 6A, C, and D), the $n(r)$ of the H1-1918, H1-1930, and H1-2005 show a higher average number of water molecules located around this glycan unit than that detected in the H1-2009. In other words, the SIA1 of the hHAR in the HA−hHAR complex of the H1-2009 virus is less solvated than that with the other three HAs. This is consistent with the hydrogen bond

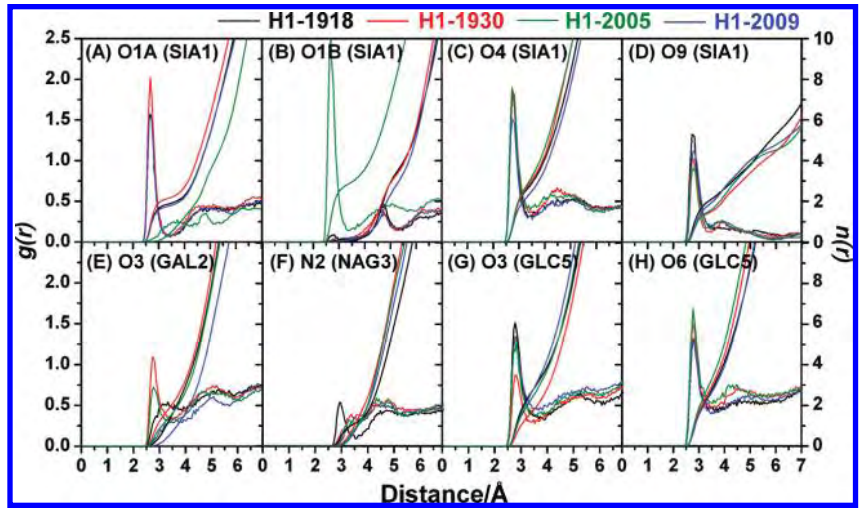

Figure 6. Radial distribution function, $g(r)$, centered on the selected heteroatoms of the hHAR (see Figure 2 for atomic labels) to oxygen atoms of water molecules and the running coordination number, $n(r)$, for the four simulated HA−hHAR systems.

data (Figure 4), where a greater level of direct contact leads to the formation of more hHAR−HA hydrogen bonds with the H1-2009 than with the other three viral strains. A clear example is the moderate hydrogen bonding between the O4 atom of SIA1 of the hHAR and the guanidinium group of the HA K145 residue that only takes place in H1-2009 (Figure 4D). Another example that supports the degree of the solvation of O9 atom (Figure 6D) is the strong hydrogen bonding between this oxygen and the HA H183 residue, which is in a reverse order of the first shell coordination numbers for O9 of 1.5 1.5, 2.0, and 2.5 water molecules for H1-2005, H1-1930, H1-2009, and H1-1918, respectively.

For the other four glycan units, the following significant differences were found: O3 of GAL2 (Figure 6E), N2 of NAG3 (Figure 6F), and O3 of GLC5 (Figure 6G), in which the degree of solvation also supports the hydrogen bond data discussed previously (Figure 4).

CONCLUSION

In the present work, MD simulations of the hHAR bound to the four different HAs of the 1918-, 1930-, 2005-, and 2009-H1N1 influenza viruses were studied and compared in terms of hydrogen bond formation, receptor conformational changes, the role of the receptor binding residues and the receptor solvation level.

In all complexes, the glycosidic torsion angle linking the terminal sialic acid and the adjoining GAL2 of apprximately −65° confirmed the preferentially favorable cis-conformation of the hHAR, similar to that detected with other HA strains.[34,35] The SIA1 terminus was found to interact strongly with the HA Y95 residue and with the conserved residues of the HA receptor binding domain, which consists of the 130-loop (V135, T136 and A137), 190-helix (H183, except for H1-1918), and 220-loop (K222 and Q226) through many strong hydrogen bonds, whereas the GAL2 and the last three glycan units (NAG3, GAL4 and GLC5) of the hHAR established hydrogen bonds with amino acids in the HA 220-loop and 190-helix, respectively. More importantly, the crucial presence of a positively charged K145 residue in the HA of the novel H1-2009 can potentially make a lysine fence with residues K133, K156, and K222 and provides an optimal contact to hydrogen bond with the SIA1 of the hHAR. Because of the presence of an uncharged S/S/N145 residue in place of the K145, such an ionic network was not created in the Spanish 1918, swine 1930, or seasonal 2005 virions, resulting in the lower potency of HA−hHAR binding. As observed in the all H1N1 strains,[15,18,20] HA residue 225 plays a critical role in the hHAR GAL2 binding efficiency. The presence of a negatively charged D225 residue in the HAs of the H1-1918 and H1-2009 could provide a larger number of hydrogen bonds in the HA−hHAR complex than that observed in H1-1930 and H1-2005, where a noncharged G225 residue exists instead. Q226 of the QAG (1918-, 1930-, and 2005-H1N1) or QEG (2009-H1N1) HA sequence directly interacts with the hHAR SIA1 terminus via hydrogen bonds, while the nonconserved 227 residue was found to play a role in stabilizing the enzyme structure around the K222 residue. Introduction of the negatively charged HA E227 residue in the H1-2009 substantially enhanced the HA−hHAR binding efficiency through hydrogen bonds formation between the HA K222 residue and the GAL2 unit of the hHAR. The lower hydrogen bonding interactions in the H1-1918, H1-1930, and H1-2005 HAs were compensated by a higher degree of water accessibility to the hHAR.

In conclusion, the efficiency of the hHAR binding to the HA of the novel 2009 H1N1 viral strain is greater than that in the 1918 Spanish and the 2005 seasonal (which is comparable to the 1930 swine) influenza viruses, respectively. A major contribution to the virion HA-cellular hHAR binding in H1-2009 is apparently gained from the charged residues existing in the HA binding pocket. Our simulated results provide a better understanding of how the viral surface glycoprotein HA of different H1N1 strains efficiently attach and bind to the hHAR.

ACKNOWLEDGMENT

This work was financially supported by the Thailand Research Fund (TRF), the Commission Higher Education (CHE), and the Thai Government Stimulus Package 2 (TKK2555), under the Project for Establishment of Comprehensive Center for Innovative Food, Health Products and Agriculture. N.N. (grant No. MRG5180298) and T.R. (grant No. TRG5280035) acknowledge the TRF grant for the new research. P.S. gratefully acknowledges the support from the Emerging Diseases and Bio-Warefare project, the Center of Excellence in Clinical Virology, Chulalongkorn University.

Supporting Information Available: Multiple sequence alignment of all four H1N1 strains and hydrogen bond descriptions. This information is available free of charge via the Internet at http://pubs.acs.org/.

REFERENCES AND NOTES

(1) World Health Organization. Global Alert and Response (GAR). http://www.who.int/csr/disease/swineflu/en/index.html (accessed July 10, 2010).

(2) Neumann, G.; Noda, T.; Kawaoka, Y. Emergence and pandemic potential of swine-origin H1N1 influenza virus. *Nature* **2009**, *459*, 931–939.

(3) Shen, J.; Ma, J.; Wang, Q. Evolutionary trends of A(H1N1) influenza virus hemagglutinin since 1918. *PLoS One* **2009**, *4*, e7789.

(4) Krug, R. M.; Aramini, J. M. Emerging antiviral targets for influenza A virus. *Trends Pharmacol. Sci*. **2009**, *30*, 269–277.

(5) Chandrasekaran, A.; Srinivasan, A.; Raman, R.; Viswanathan, K.; Raguram, S.; Tumpey, T. M.; Sasisekharan, V.; Sasisekharan, R. Glycan topology determines human adaptation of avian H5N1 virus hemagglutinin. *Nat. Biotechnol*. **2008**, *26*, 107–113.

(6) Bateman, A. C.; Busch, M. G.; Karasin, A. I.; Bovin, N.; Olsen, C. W. Amino acid 226 in the hemagglutinin of H4N6 influenza virus determines binding affinity for 2,6-linked sialic acid and infectivity levels in primary swine and human respiratory epithelial cells. *J. Virol*. **2008**, *82*, 8204–8209.

(7) Gambaryan, A. S.; Karasin, A. I.; Tuzikov, A. B.; Chinarev, A. A.; Pazyninab, G. V.; Bovinb, N. V.; Matrosovich, M. N.; Olsen, C. W.; Klimove, A. I. Receptor-binding properties of swine influenza viruses isolated and propagated in MDCK cells. *Virus. Res*. **2005**, *114*, 15–22.

(8) Matrosovich, M. N.; Gambaryan, A. S.; Teneberg, S.; Piskarev, V. E.; Yamnikova, S. S.; Lvov, D. K.; Robertson, J. S.; Karlsson, K. A. Avian influenza A viruses differ from human viruses by recognition of sialyloligosaccharides and gangliosides and by a higher conservation of the HA receptor-binding site. *Virology* **1997**, *23*, 224–234.

(9) Rogers, G. N.; D'Souza, B. L. Receptor binding properties of human and animal H1 influenza virus isolates. *Virology* **1989**, *173*, 317–322.

(10) Bewley, C. A. Illuminating the switch in influenza viruses. *Nat. Biotechnol*. **2008**, *26*, 60–62.

(11) Laohpongspaisan, C.; Rungrotmongkol, T.; Intharathep, P.; Malaisree, M.; Decha, P.; Aruksakunwong, O.; Sompornpisut, P.; Hannongbua, S. Why amantadine loses its function in influenza M2 mutants: MD simulations. *J. Chem. Inf. Model*. **2009**, *49*, 847–852.

(12) Ghosh, A.; Nandy, A.; Nandy, P.; Gute, B. D.; Basak, S. C. Computational study of dispersion and extent of mutated and duplicated sequences of the H5N1 influenza neuraminidase over the period 1997−2008. *J. Chem. Inf. Model*. **2009**, *49*, 2627–2638.

(13) Udommaneethanakit, T.; Rungrotmongkol, T.; Bren, U.; Frecer, V.; Stanislav, M. Dynamic behavior of avian influenza A virus neuraminidase subtype H5N1 in complex with oseltamivir, zanamivir, peramivir, and their phosphonate analogues. *J. Chem. Inf. Model*. **2009**, *49*, 2323–2332.

(14) Rungrotmongkol, T.; Intharathep, P.; Malaisree, M.; Nunthaboot, N.; Kaiyawet, N.; Sompornpisut, P.; Payungporn, S.; Poovorawan, Y.; Hannongbua, S. Susceptibility of antiviral drugs against 2009 influenza A (H1N1) virus. *Biochem. Biophys. Res. Commun*. **2009**, *385*, 390–394.

(15) Glaser, L.; Stevens, J.; Zamarin, D.; Wilson, I. A.; García-Sastre, A.; Tumpey, T. M.; Basler, C. F.; Taubenberger, J. K.; Palese, P. A single amino acid substitution in 1918 influenza virus hemagglutinin changes receptor binding specificity. *J. Virol*. **2005**, *79*, 11533–11536.

(16) Stevens, J.; Blixt, O.; Tumpey, T. M.; Taubenberger, J. K.; Paulson, J. C.; Wilson, I. A. Structure and receptor specificity of the hemagglutinin from an H5N1 influenza virus. *Science* **2006**, *312*, 404–410.

(17) Taubenberger, J. K. Influenza hemagglutinin attachment to target cells: "Birds do it, we do it". *Future Virol*. **2006**, *1*, 415–418.

(18) Matrosovich, M.; Tuzikov, A.; Bovin, N.; Gambaryan, A.; Klimov, A.; Castrucci, M. R.; Donatelli, I.; Kawaoka, Y. Early alterations of the receptor-binding properties of H1, H2, and H3 avian influenza virus hemagglutinins after their introduction into mammals. *J. Virol*. **2000**, *74*, 8502–8512.

(19) Yang, Z. Y.; Wei, C. J.; Kong, W. P.; Wu, L.; Xu, L.; Smith, D. F.; Nabel, G. J. Immunization by avian H5 influenza hemagglutinin mutants with altered receptor binding specificity. *Science* **2007**, *317*, 825–828.

(20) Stevens, J.; Blixt, O.; Glaser, L.; Taubenberger, J. K.; Palese, P.; Paulson, J. C.; Wilson, I. A. Glycan microarray analysis of the hemagglutinins from modern and pandemic influenza viruses reveals different receptor specificities. *J. Mol. Biol*. **2006**, *355*, 1143–1155.

(21) Gamblin, S. J.; Haire, L. F.; Russell, R. J.; Stevens, D. J.; Xiao, B.; Ha, Y.; Vasisht, N.; Steinhauer, D. A.; Daniels, R. S.; Elliot, A.; Wiley, D. C.; Skehel, J. J. The structure and receptor-binding properties of the 1918 influenza hemagglutinin. *Science* **2004**, *303*, 1838–1842.

(22) Nunthaboot, N.; Rungrotmongkol, T.; Malaisree, M.; Decha, P.; Kaiyawet, N.; Intharathep, P.; Sompornpisut, P.; Poovorawan, Y.; Hannongbua, S. Molecular insights into human receptor binding to 2009 H1N1 influenza A hemagglutinin. *Monatsh. Chem*. **2010**, *141*, 801–807.

(23) Influenza virus resource. http://www.ncbi.nlm.nih.gov/genomes/FLU/SwineFlu.html (accessed Apr 25, 2009).

(24) *Discovery Studio 2.0*; Accelrys Inc: San Diego, CA, 2007.

(25) Case, D. A.; Darden, T. A.; Cheatham, III, T. E.; Simmerling, C. L.; Wang, J.; Duke, R. E.; Luo, R.; Crowley, M.; Walker, R. C.; Zhang, W.; Merz, K. M.; Wang, B.; Hayik, S.; Roitberg, A.; Seabra, G.; Kolossváry, I.; Wong, K. F.; Paesani, F.; Vanicek, J.; Wu, X.; Brozell, S. R.; Steinbrecher, T.; Gohlke, H.; Yang, L.; Tan, C.; Mongan, J.; Hornak, V.; Mathews, G. C. D. H.; Seetin, M. G.; Sagui, C.; Babin, V.; Kollman, P. A. *AMBER10*; University of California: San Francisco, CA, 2008.

(26) Duan, Y.; Wu, C.; Chowdhury, S.; Lee, M. C.; Xiong, G.; Zhang, W.; Yang, R.; Cieplak, P.; Luo, R.; Lee, T.; Caldwell, J.; Wang, J.; Kollman, P. A point-charge force field for molecular mechanics simulations of proteins based on condensed-phase quantum mechanical calculations. *J. Comput. Chem*. **2003**, *24*, 1999–2012.

(27) Tessier, M. B.; Demarco, M. L.; Yongye, A. B.; Woods, R. J. Extension of the GLYCAM06 biomolecular force field to lipids, lipid bilayers and glycolipids. *Mol. Simulat*. **2008**, *34*, 349–364.

(28) Li, H.; Robertson, A. D.; Jensen, J. H. Very fast empirical prediction and rationalization of protein pKa values. *Proteins* **2005**, *61*, 704–721.

(29) Bas, D. C.; Rogers, D. M.; Jensen, J. H. Very fast prediction and rationalization of pKa values for protein-ligand complexes. *Proteins* **2008**, *73*, 765–783.

(30) Darden, T.; York, D.; Pedersen, L. Particle mesh Ewald: an N-log(N) method for Ewald sums in large systems. *J. Chem. Phys*. **1993**, *98*, 10089–10092.

(31) Ryckaert, J.; Ciccotti, G.; Berendsen, H. J. C. Numerical integration of the cartesian equations of motion of a system with constraints: Molecular dynamics of *n*-alkanes. *J. Comput. Phys*. **1977**, *23*, 327–341.

(32) Lin, T.; Wang, G.; Li, A.; Zhang, Q.; Wu, C.; Zhang, R.; Cai, Q.; Song, W.; Yuen, K. Y. The hemagglutinin structure of an avian H1N1 influenza A virus. *Virology* **2009**, *392*, 73–81.

(33) Kumari, K.; Gulati, S.; Smith, D. F.; Gulati, U.; Cummings, R. D.; Air, G. M. Receptor binding specificity of recent human H3N2 influenza viruses. *Virol. J*. **2007**, *4*, 42–53.

(34) Li, M.; Wang, B. Computational studies of H5N1 hemagglutinin binding with SA-alpha-2, 3-Gal and SA-α-2, 6-Gal. *Biochem. Biophys. Res. Commun*. **2006**, *347*, 662–668.

(35) Xu, D.; Newhouse, E. I.; Amaro, R. E.; Pao, H. C.; Cheng, L. S.; Markwick, P. R.; McCammon, J. A.; Li, W. W.; Arzberger, P. W. Distinct glycan topology for avian and human sialopentasaccharide receptor analogues upon binding different hemagglutinins: A molecular dynamics perspective. *J. Mol. Biol*. **2009**, *387*, 465–491.

(36) Soundararajan, V.; Tharakaraman, K.; Raman, R.; Raguram, S.; Shriver, Z.; Sasisekharan, V.; Sasisekharan, R. Extrapolating from sequence-the 2009 H1N1 "swine" influenza virus. *Nat. Biotechnol*. **2009**, *27*, 510–513.

(37) Coburn, B. J.; Wagner, B. G.; Blower, S. Modeling influenza epidemics and pandemics: insights into the future of swine flu (H1N1). *BMC. Med*. **2009**, *7*, 30–37.

(38) Munster, V. J.; de Wit, E.; van den Brand, J. M.; Herfst, S.; Schrauwen, E. J.; Bestebroer, T. M.; van de Vijver, D.; Boucher, C. A.; Koopmans, M.; Rimmelzwaan, G. F.; Kuiken, T.; Osterhaus, A. D.; Fouchier, R. A. Pathogenesis and transmission of swine-origin 2009 A(H1N1) influenza virus in ferrets. *Science* **2009**, *325*, 481–483.

(39) Maines, T. R.; Jayaraman, A.; Belser, J. A.; Wadford, D. A.; Pappas, C.; Zeng, H.; Gustin, K. M.; Pearce, M. B.; Viswanathan, K.; Shriver, Z. H.; Raman, R.; Cox, N. J.; Sasisekharan, R.; Katz, J. M.; Tumpey, T. M. Transmission and pathogenesis of swine-origin 2009 A(H1N1) influenza viruses in ferrets and mice. *Science* **2009**, *325*, 484–487.

(40) Chen, J.; Fang, F.; Yang, Z.; Liu, X.; Zhang, H.; Zhang, Z.; Zhang, X.; Chen, Z. Characterization of highly pathogenic H5N1 avian influenza viruses isolated from poultry markets in central China. *Virus. Res*. **2009**, *146*, 19–28.

CI100038G

Effects of Residues Changes on Human Receptor Binding Affinity of H1N1 Hemagglutinins: Insights from Molecular Dynamics Simulation

N. Nunthaboot[1,C], T. Rungrotmongkol[2,3], M. Malaisree[2], N. Kaiyawet[2], P. Decha[4], P. Sompornpisut[2] and S. Hannongbua[2,C]

[1]*Department of Chemistry, Faculty of Science, Mahasarakham University, Mahasarakham, Thailand*
[2]*Department of Chemistry, Faculty of Science, Chulalongkorn University, Bangkok, Thailand*
[3]*Center of Innovative Nanotechnology, Chulalongkorn University, Bangkok, Thailand*
[4]*Department of Chemistry, Faculty of Science, Thaksin University, Phattalung, Thailand*
[C]**E-mail**: nadtanet@gmail.com, supot.h@chula.ac.th; **Fax:** 02-2187603; **Tel.** 02-2187603

ABSTRACT

The recent outbreak of the novel 2009 H1N1 influenza in humans has focused global attention on this virus which could potentially have introduced a more dangerous pandemic of influenza flu. In the initial step of the viral attachment, hemagglutinin (HA), a viral glycoprotein surface, is responsible for the binding to the human SIA α2,6 linked sialopentasaccharide host cell receptor (hHAR). Dynamic and structural properties, based on molecular dynamics simulations of the three different HAs of Spanish 1918 (H1-1918), swine 1930 (H1-1930) and the novel 2009 (H1-2009) H1N1 bound to the hHAR, were compared. In all three HA – hHAR complexes, major interactions with the receptor binding were gained from HA residue Y95 and the conserved HA residues of the 130-loop, 190-helix and 220-loop. However, substitution of the charged HA residues K145 and E227 into the 2009 HA binding pocket was found to increase the HA - hHAR binding efficiency in comparison to the two previously recognized H1N1 strains. Changing of the non-charged HA G225 residue to a negatively charged D225 provides a larger number of hydrogen bonding interactions. The increase in hydrophilicity of the receptor binding region is apparently an evolutionary trend of the current pandemic flu from the 1918 Spanish and 1930 swine flues. Detailed analysis could help the understanding of how different HA effectively attaches and binds with the hHAR.

Keywords: H1N1, Hemagglutinin, sialopentasaccharide**,** Molecular Dynamics

REFERENCES

1. Soundararajan, V., Tharakaraman, K., Raman, R., Raguram, S., Shriver, Z., Sasisekharan, V., and Sasisekharan, R. *Nat. Biotechnol*., 2009, 27, 510-513.
2. Stevens, J., Blixt, O., Tumpey, T. M., Taubenberger, J. K., Paulson, J. C., and Wilson, I. A. *Science*, 2006, 312, 404-410.
3. Gamblin, S. J., Haire, L. F., Russell, R. J., Stevens, D. J., Xiao, B., Ha, Y., Vasisht, N., Steinhauer, D. A., Daniels, R. S., Elliot, A., Wiley, D. C., and Skehel, J. J. *Science*, 2004, 303, 1838-1842

Changes of human receptor binding affinity of H1N1 hemagglutinins: Insights from molecular dynamics simulation

N. Nunthaboot[1,C], T. Rungrotmongkol[2,3], M. Malaisree[2], N. Kaiyawet[2], P. Decha[4], P. Sompornpisut[2] and S. Hannongbua[2,C]

[1]*Department of Chemistry, Faculty of Science, Mahasarakham University, Mahasarakham, Thailand*
[2]*Department of Chemistry, Faculty of Science, Chulalongkorn University, Bangkok, Thailand*
[3]*Center of Innovative Nanotechnology, Chulalongkorn University, Bangkok, Thailand*
[4]*Department of Chemistry, Faculty of Science, Thaksin University, Phattalung, Thailand*
[C]**E-mail**: nadtanet@gmail.com, supot.h@chula.ac.th; **Fax:** 02-2187603; **Tel.** 02-2187603

The binding of the viral glycoprotein, hemagglutinin (HA), and the human-α2,6-linked sialopentasaccharide host cell receptor (hHAR) is a critical step in the viral replication cycle. Dynamical and structural properties of the four different HAs of Spanish 1918 (H1-1918), swine 1930 (H1-1930), seasonal 2005 (H1-2005) and a novel 2009 (H1-2009) H1N1 bound to the hHAR, were investigated by means of molecular dynamics simulations. In all systems, major interactions between HA residues and hHAR were obtained from Y95 and the conserved residues of the 130-loop, 190-helix and 220-loop. Compared to the three previously recognized H1N1 strains, introductions of K145 and E227, charged residues, increased the HA-hHAR binding efficiency of 2009 HA H1N1. In addition, changing of G225, the non-charged residue, to D225, a negatively charged residue, provides a larger number of hydrogen bonding interactions. The obtained information could help the understanding of how different HAs effectively attach and bind with the hHAR.

Keywords: H1N1, Hemagglutinin, Human Receptor**,** Molecular Dynamics

References

1. Soundararajan, V., Tharakaraman, K., Raman, R., Raguram, S., Shriver, Z., Sasisekharan, V., and Sasisekharan, R. *Nat. Biotechnol*., 2009, 27, 510-513.
2. Stevens, J., Blixt, O., Tumpey, T. M., Taubenberger, J. K., Paulson, J. C., and Wilson, I. A. *Science*, 2006, 312, 404-410.
3. Gamblin, S. J., Haire, L. F., Russell, R. J., Stevens, D. J., Xiao, B., Ha, Y., Vasisht, N., Steinhauer, D. A., Daniels, R. S., Elliot, A., Wiley, D. C., and Skehel, J. J. *Science*, 2004, 303, 1838-1842

BIOGRAPHY

PERSONAL DATA

Name: Nadtanet Nunthaboot

Gender: Female

Status: Single

Current position Lecturer

Current Address: 4th Floor, Room 414, Science (1) Building
Department of Chemistry, Faculty of Science
Mahasarakham University, Kham-Riang Campus
Kuntara-Wichai, Mahasarakham, 44150, Thailand

Date of birth: 11 April 1980

Place of birth: Ubonratchathani, Thailand

Nationality: Thai

Office phone number: (66)-43 -754246

Office fax number: (66)-43- 754246

E-mail address: nadtanet@gmail.com

EDUCATION

2007-present:

Lecturer, Mahasarakham University, Mahasarakham, Thailand

2002-2007:

Ph.D. Candidate**,** Computational Chemistry, Chulalongkorn University, Thailand

Ph. D. Project: 3D-QSAR and Molecular Dynamics Simulations of HIV-1 integrase and its complex with inhibitors

Supervisor: Assoc. Prof. Dr. Sirirat Kokpol

Degree received: May 2007

1998-2002:

B.Sc. Chemistry, Khon Kaen University, Thailand

Project: Study of Aluminum Clusters by Quantum Chemical Calculations

Supervisor: Assoc. Prof. Dr. Sunantha Hengrasmee

Degree received: May 2002

LANGUAGES:

Thai – native

English – fluently

German – basic conversation

GRANTS:

1. Scholarship from the Thailand Research Fund (TRF), 2008-present
2. Fulbright –TRF Thai Junior Research Scholarship Program (2005), 2005-2006
3. The Royal Golden Jubilee Ph.D. Scholarship, Thailand Research Fund, 2002-2007

PROFESSIONAL SOCIETY:

American Chemical Society, member

AREA OF INTERESTS

- Quantum Chemistry and QM/MM Calculations
- Molecular Dynamics Simulation
- Binding Free Energy Calculation using MM-PB(GB)SA method
- Computer Aided Molecular (Drug) Design
- Bioinformatics

COMPUTATIONAL SKILLS

- Computational Chemistry, Molecular Modeling and Drug Design software packages such as Gaussian, MOPAC, GAMESS, CHARMM, AMBER, SYBYL, Insight II, Autodock, DRAGON, MOE
- Unix and Windows operating system

ACTIVITIES AND RESEARCH VISITING

1. Participate in the 1st Thai Summer School, Khon Kaen University, Thailand, 2003.
2. Participate in RGJ-PhD. Congress IV, Chonburi, Thailand, 2003.
3. Visiting scholar at Wolschann's group (QSAR technique), University of Vienna, Vienna, Austria, 2004.
4. Visiting scholar at Briggs's Group (QM/MM technique), University of Houston, Houston, TX, USA, 2005-2006.
5. Participate in the 2006 Fulbright Visiting Scholar Conference: The Rule of Law in the United States, Denver, Colorado, USA, 2006.
6. Participate in the 11th Structural Biology Symposium, The University of Texas Medical Branch at Galveston, Galveston, Texas, USA, 2006.
7. Participate in the 5th Thai Summer School, Suranaree University of Technology, Thailand, 2008.
8. Fellow at International Centre for Science and High Technology, UNIDO, AREA Science Park, Trieste, Italy

CONFERENCES and PRESENTATIONS:

Poster Presentations

1. Potential Energy Surface Studies of 4 – aryl - 2, 4 - dioxobutanoic acid compounds, The 29th Conference of Science and Technology of Thailand (STT29), Khon Kaen, Thailand, 2002.
2. Quantitative Structure Activity Relationships Studies on HIV-1 Integrase Inhibitors using CoMFA and CoMSIA, The QSAR EURO, Istanbul, Turkey, 2004.
3. Conformation of Derivatives of 4-Aryl-2, 4-dioxobutanoic acid: A Class of HIV-1 Integrase inhibitor, The 2nd Asian Pacific Conference on Theoretical & Computational Chemistry (APCTCC), Bangkok, Thailand, 2005.
4. CoMFA and CoMSIA 3D-QSAR study of HIV-1 Integrase Inhibitors, The 2nd Asian Pacific Conference on Theoretical & Computational Chemistry (APCTCC), Bangkok, Thailand, 2005.

5. Three-Dimensional Quantitative Structure-Activity Relationship (3D-QSAR) Studies of HIV-1 Integrase Inhibitors, The RGJ-PhD. VI Congress, Chonburi, Thailand, 2005.

6. Docking calculations on HIV-1 integrase inhibitors: insight in to the binding modes of diketo acids, The 31st Conference of Science and Technology of Thailand (STT31), Nakorn Ratchasrima, Thailand, 2005.

7. Investigation of metal dependent behavior of HIV-1 integrase inhibitors: DFT calculation, American Chemical Society National Meeting, Atlanta, Georgia, USA, 2006.

8. Comparison of QM/MM and MM Force Fields in MD simulations of HIV-1 Integrase-5CITEP System. American Chemical Society Western Regional Meeting 2007 Frontiers in Chemistry, Biopharmaceuticals & Biotechnology. San Diego, CA, USA. 2007.

9. Computer-Aided Drug Design of HIV-1 Integrase Inhibitors: Three-Dimensional Quantitative Structure Activity Relationship Study, Molecular Design and Computer-assisted Combinatorial Chemistry, Trieste, Italy. 2008.

10. Dynamics of Photoinduced Charge Transfer Interaction in FMN binding Protein. Pure and Applied Chemistry International Conference. Department of Chemistry, Faculty of Science, Naresuan University. 2009.

11. Correlation between Photoinduced Electron Transfer Rate and Structural Factors in FMN Binding Protein. Pure and Applied Chemistry International Conference. Department of Chemistry, Faculty of Science, Naresuan University. 2009.

12. Molecular insights of human receptor binding to 2009 H1N1 influenza A hemagglutinin. การประชุมนักวิจัยรุ่นใหม่พบเมธีวิจัยอาวุโส สกว. ครั้งที่ 9 ณ โรงแรมฮอลิเดย์อินน์ รีสอร์ท รีเจนท์ บีช ชะอำ 2009.

Oral Presentations:

1. 3D-QSAR CoMFA and CoMSIA on HIV-1 Integrase inhibitors, Joint Meeting of the Austrian, Czech and German Pharmaceutical Societies, Regensburg, Germany, 2004.

2. Comparative molecular field analysis and comparative molecular similarity indices analysis of HIV-1 integrase inhibitors, The 9th Annual National Symposium on Computational Science and Engineering (ANSCSE 9), Bangkok, Thailand. 2005.

3. A QSAR study of diverse structural classes of HIV-1 Integrase Inhibitors, Thai-Austria Theoretical Chemistry Collaboration: A Successful Interdisciplinary Cooperation, Bangkok, Thailand, 2006.

4. Binding Interaction between HIV-1 Integrase and Lithospermic Acid: A Computational Docking Study, The 11th Annual National Symposium on Computational Science and Engineering (ANSCSE 11), Prince of Songkla University, Phuket campus, Phuket, Thailand. 2007.

5. Insight into Specific Binding of Hemagglutinin with SA-alpha-2,3-Gal and SA-alpha-2,6-Gal: QM/MM MD Simulations, Global Concerns, Recent Outbreak and Molecular Insight into Avian Influenza H5N1, Bangkok, Thailand**,** 2008.

6. Effects of Residues Changes on Human Receptor Binding Affinity of H1N1 Hemagglutinins: Insights from Molecular Dynamics Simulation. 14th International Annual Symposium on Computational Science and Engineering (ANSCSE14)**.** Mae Fah Luang University**.** Chiang Rai. 2010

7. Changes of human receptor binding affinity of H1N1 hemagglutinins: Insights from molecular dynamics simulation. 240th American Chemical Society National Meeting. Boston, MA, USA, 2010.

PUBLICATIONS:

1**.** Nadtanet Nunthaboot, Somsak Tonmunphean, Vudhichai Parasuk, Peter Wolschann, and Sirirat Kokpol. Three-Dimensional Quantitative Structure Activity Relationships Studies on Diverse Structural Classes of HIV-1 Integrase Inhibitors using CoMFA and CoMSIA. *European Journal of Medicinal Chemistry*. 41, 1359-1372, 2006.

2. Nadtanet Nunthaboot, Somsak Pianwanit, Vudhichai Parasuk, Sirirat Kokpol, and James M. Briggs. Computational studies of HIV-1 integrase and its inhibitors. *Current Computer-Aided Drug Design.* 3, 160-190, 2007.

3. Nadtanet Nunthaboot, Somsak Painwanit, Vudhichai Parasuk, Sirirat Kokpol, and Peter Wolschann. Theoretical study on the HIV-1 integrase inhibitor 1-(5-chloroindol-3-yl)-3-hydroxy-3-(2H-tetrazol-5-yl)-propenone (5CITEP). *Journal of Molecular Structure*. 844-845, 208-214, 2007.

4. Nadtanet Nunthaboot, Jerry O. Ebalunode, Somsak Painwanit, Vudhichai Parasuk, James M. Briggs and Sirirat Kokpol. Hybrid Quantum Mechanical/Molecular Mechanical Molecular Dynamics Simulations of HIV-1 Integrase/Inhibitor Complexes. *Biophysical Journal*. 93, 3613-3626, 2007.

5. Nadtanet Nunthaboot, Fumio Tanaka, Sirirat Kokpol, Haik Chosrowjan, Seiji Taniguchi, and Noboru Mataga. Simultaneous Analysis of Ultrafast Fluorescence Decays of FMN Binding Protein and Its Mutated Proteins by Molecular Dynamic Simulation and Electron Transfer Theory. *Journal of Physical Chemistry B.* 112, 13121-13127, 2008.

6. Nadtanet Nunthaboot, Fumio Tanaka, Sirirat Kokpol, Haik Chosrowjan, Seiji Taniguchi, Noboru Mataga. Quantum Mechanical Study of Photoinduced Charge Transfer in FMN Binding Protein. *Journal of Physical Chemistry B.*112, 15837-15843, 2008.

7. Nadtanet Nunthaboot, Fumio Tanaka, Sirirat Kokpol, Haik Chosrowjan, Seiji Taniguchi, Noboru Mataga. Simulation of ultrafast non-exponential fluorescence decay induced by electron transfer in FMN binding protein. *Journal of Photochemistry and Photobiology A: Chemistry*. 201, 191-196, 2008.

8. Thanyada Rungrotmongkol, Panita Decha, Pornthep Sompornpisut, Maturos Malaisree, Pathumwadee Intharathep, Nadtanet Nunthaboot, Thanyarat Udommaneethanakit, Ornjira Aruksakunwong, Supot Hannongbua. Combined QM/MM mechanistic study of the acylation process in furin complexed with the H5N1 avian influenza virus hemagglutinin's cleavage site. *Proteins*. 76, 62-71, 2008.

9. Maturos Malaisree, Thanyada Rungrotmongkol, Nadtanet Nunthaboot, Ornjira Aruksakunwong, Pathumwadee Intharathep, Panita Decha, Pornthep Sompornpisut, Supot Hannongbua. Source of Oseltamivir Resistance in Avian Influenza H5N1 Viruses with the H274Y Mutation. *Amino Acids*. *37*, 725-732, 2009.

10. Thanyada Rungrotmongkol, Pathumwadee Intharathep, Maturos Malaisree, Nadtanet Nunthaboot, Nopphorn Kaiyawet, Pornthep Sompornpisut, Sanchai Payungporn, Yong Poovorawan and Supot Hannongbua. Susceptibility of antiviral drugs against 2009 influenza A (H1N1) virus. *Biochemical and Biophysical Research Communications. 385*, 390-394, 2009.

11. Banchob Wanno, Wandee Rakrai, Somchai Keawwangchai, Neramit Morakot, Nongnit Morakot, Nadtanet Nunthaboot, Vithaya Ruangpornvisuti. A density functional investigation of 1,3-bis(4-nitrophenyl)urea as anion receptor. J*ournal of Molecular Structure: THEOCHEM*. *902*, 33-40, 2009.

12. Nadtanet Nunthaboot Fumio Tanaka, Sirirat Kokpol. Analysis of Photoinduced Electron Transfer in AppA. *Journal of Photochemistry and Photobiology A: Chemistry. 207*, 274-281, 2009.

13. Thanyada Rungrotmongkol, Thanyarat Udommaneethanakit, Maturos Malaisree, Nadtanet Nunthaboot, Pathumwadee Intharathep, Pornthep Sompornpisut and Supot Hannongbua. How does each substituent functional group of oseltamivir lose its activity against virulent H5N1 influenza mutants? *Biophysical Chemistry. 145*, 29-36, 2009.

14. Fumio Tanana and Nadtanet Nunnthaboot. Correlation between photoinduced electron transfer rate and structural factors in FMN binding protein. *Proceeding: Pure and Applied Chemistry International Conference*. 491-494, 2009.

15. Nadtanet Nunnthaboot and Fumio Tanana. Dynamic of photoinduced charge transfer interaction in FMN binding protein. *Proceeding: Pure and Applied Chemistry International Conference*. 495-499, 2009.

16. Thanyada Rungrotmongkol, Maturos Malaisree, Nadtanet Nunthaboot, Pornthep Sompornpisut, and Supot Hannongbua. Molecular Prediction of Oseltamivir Efficiency against Probable Influenza A (H1N1-2009) Mutants: Molecular Modelling Approach. *Amino Acids*. *39*, 393-398. 2010.

17. Nadtanet Nunthaboot, Thanyada Rungrotmongkol, Maturos Malaisree, Panita Decha, Nopphorn Kaiyawet, Pathumwadee Intharathep, Pornthep Sompornpisut, Yong Poovorawan and Supot Hannongbua. Molecular insights into human receptor binding to 2009 H1N1 influenza A hemagglutinin. *Monatshefte für Chemie. 141*, 801-807, 2010.

18. Nadtanet Nunthaboot, Thanyada Rungrotmongkol, Maturos Malaisree, Nopphorn Kaiyawet, Panita Decha, Pornthep Sompornpisut, Yong Poovorawan and Supot Hannongbua. Evolution of Human Receptor Binding Affinity of H1N1 Hemagglutinins from 1918 to 2009 Pandemic Influenza A Virus. *Journal of Chemical Information and Model*ing, *50*, 1410-1417, 2010.

19. Nadtanet Nunthaboot, Fumio Tanaka, Sirirat Kokpol. Simultaneous analysis of photoinduced electron transfer in wild type and mutated AppAs. *Journal of Photochemistry and Photobiology A: Chemistry*. *20*9, 79-87, 2010.

20. Rong Rujkorakarn, Nadtanet Nunthaboot, Fumio Tanaka, Pimchai Chaiyen, Haik Chosrowjan, Seiji Taniguchi, Noboru Mataga. Time-resolved Stokes shift in proteins with continuum model: Slow dynamics in proteins. *Journal of Photochemistry and Photobiology A: Chemistry*. *In press*. 2010.

21. Pathumwadee Intharathep, Thanyada Rungrotmongkol, Panita Decha, Nadtanet Nunthaboot, Nopphorn Kaiyawet, Teerakiat Kerdcharoen, Pornthep Sompornpisut, Supot Hannongbua. Evaluating how rimantadines control the proton gating of the influenza A M2-proton port via allosteric binding outside of the M2-channel: MD simulations. *Journal of Enzyme Inhibition and Medicinal Chemistry*, *In press*, 2010.